

Rochester Institute of Technology

## RIT Scholar Works

---

### Theses

---

6-1-2000

## A Theoretical model showing the effects of the fuel induced gamma effect

Bryan Bordeleau

Follow this and additional works at: <https://scholarworks.rit.edu/theses>

---

### Recommended Citation

Bordeleau, Bryan, "A Theoretical model showing the effects of the fuel induced gamma effect" (2000). Thesis. Rochester Institute of Technology. Accessed from

This Thesis is brought to you for free and open access by RIT Scholar Works. It has been accepted for inclusion in Theses by an authorized administrator of RIT Scholar Works. For more information, please contact [ritscholarworks@rit.edu](mailto:ritscholarworks@rit.edu).

# **A THEORETICAL MODEL SHOWING THE EFFECTS OF THE FUEL INDUCED GAMMA EFFECT**

Bryan A. Bordeleau

Mechanical Engineering Department  
Rochester Institute of Technology  
Rochester, NY

A Thesis Submitted in  
Partial Fulfillment of the  
Requirements for the  
Degree of

MASTER OF SCIENCE  
in  
Mechanical Engineering

Approved by: Professor \_\_\_\_\_  
Dr. A. Nye, Thesis Advisor

Professor \_\_\_\_\_  
Dr. F. Sciremammano

Industry Sponsor \_\_\_\_\_  
L. Markle

Professor \_\_\_\_\_  
Dr. S. Kandlikar, Dept. Head

June 2000

**DEPARTMENT OF MECHANICAL ENGINEERING**

**COLLEGE OF ENGINEERING**

**ROCHESTER INSTITUTE OF TECHNOLOGY**

**2000**

**COPYRIGHT INFORMATION**

This volume is the property of the Institute, but the literary rights of the author must be respected. Passages must not be copied or closely paraphrased without the previous written consent of the author. If the reader obtains any assistance from this volume, he or she must give proper credit in his or her own work.

The following persons, whose signatures attest their acceptance of the above restrictions, have used this thesis:

Name and Address:

Date:

## PERMISSION TO REPRODUCE

Thesis Title: “A Theoretical Model Showing the Effects of the Fuel Induce Gamma Effect”

I, Bryan A. Bordeleau, hereby grant permission to the Wallace Memorial Library of the Rochester Institute of Technology to reproduce my thesis in whole or in part. Any reproduction can not be used commercially or for profit.

2000

## FORWARD

It has been a long and difficult process to complete this thesis. Many long hours and late nights have been spent researching and writing, and it all has been worth it. This period of time has also been difficult for those around me, especially for my friend and loving wife, Carrie. I'd like to thank her very much, for giving me all her support, love, and kindness, and for helping me every step of the way.

Also I would like to thank my Mom and Dad for all their support. They have given me guidance, encouragement, and understanding. They have instilled in me the determination to succeed in all that I do.

A special thanks goes to my grandparents, who have always supported my dreams and goals.

Without the help and knowledge of Lee Markle and Paul VanBrocklin, at Delphi Automotive Systems, this project would have never gotten off the ground.

And finally, I want to thank "Doc" Nye, for all his help and guidance. Without his knowledge and insight I would have gotten lost many times along the way.

## NOMENCLATURE

### *Symbols*

$A_s$	Surface Area [ $\text{cm}^2$ ]
$b$	y-intercept of a line [cm]
$B$	Bore [cm]
$B_p$	Bisection Method product
$C, K$	Constants
$c_p$	Specific heat at constant pressure [kJ/kg-K]
$c_v$	Specific heat at constant volume [kJ/kg-K]
$E$	Total Energy [kJ]
$h$	Specific enthalpy [kJ/kg] or cylinder height [cm]
$h_T$	Heat transfer coefficient [ $\text{kW/m}^2 \text{ K}$ ]
$L_v$	Latent heat of vaporization [kJ/kg]
$m$	Mass [kg]
$M$	Molecular weight [kg]
$p$	Pressure [kPa]
$Q$	Heat transfer [kJ]
$Q_{xy}$	Heat transfer between states x and y [kJ]
$r$	Radius [cm]
$r_v$	Compression ratio
$R$	Gas constant [kJ/kg-K]
$R_u$	Universal gas constant [kJ/kg-K]
$T$	Temperature [K]
$u$	Specific internal energy [kJ/kg]
$U$	Internal energy [kJ]
$V$	Volume [ $\text{cm}^3$ ]
$W$	Work [kJ]
$x, y$	Graphical coordinates [cm]

### *Acronyms*

BDC	Bottom Dead Center
$\text{CA}^\circ$	Crank Angle Degrees
DI-G	Direct Injection Gasoline
FIGE	Fuel Induced Gamma Effect
KE	Kinetic Energy
LIEF	Laser Induced Exciplex Fluorescence
PE	Potential Energy
TDC	Top Dead Center

### *Greek Letters*

$\Delta$	Change
$\eta_{otto}$	Otto cycle efficiency
$\gamma$	Specific heat ratio

### *Subscripts*

air	In-cylinder air
ave	Average
calc	Calculated
clear	Clearance
cyl	Cylinder
data	Experimental data
f	Final
fuel	Evaporated fuel
i	Initial
loss	Loss due to leaks
max	Maximum
min	Minimum
resid	Residual
s	Slope or Surface
tot	Total
$\infty$	Fluid

## TABLE OF CONTENTS

---

<b>COPYRIGHT INFORMATION.....</b>	<b>II</b>
<b>FORWARD.....</b>	<b>IV</b>
<b>NOMENCLATURE .....</b>	<b>V</b>
SYMBOLS.....	V
ACRONYMS .....	V
GREEK LETTERS .....	VI
SUBSCRIPTS .....	VI
<b>ABSTRACT .....</b>	<b>X</b>
<b>1. INTRODUCTION.....</b>	<b>1</b>
<b>2. THE THEORY AND HISTORY OF FUEL INJECTED INTERNAL COMBUSTION ENGINES</b>	<b>3</b>
2.1 THERMODYNAMIC THEORY .....	3
2.1.1 <i>The First Law of Thermodynamics</i> .....	3
2.1.2 <i>Ideal Gases</i> .....	4
2.1.3 <i>Heat Transfer</i> .....	8
2.1.4 <i>Work</i> .....	10
2.1.5 <i>The Otto Cycle</i> .....	11
2.2 FUEL INJECTION DEVICES.....	18
2.2.1 <i>Carburation</i> .....	18
2.2.2 <i>Port Fuel Injection</i> .....	19
2.2.3 <i>Direct Injection</i> .....	20
<b>3. STATE-OF-THE-ART FUEL QUALITY MEASUREMENT TECHNIQUES .....</b>	<b>22</b>
3.1 FIBER OPTIC SPARK PLUG PROBE.....	22
3.2 THE OPTICAL ENGINE .....	23
3.3 THE ARGON ION LASER TECHNIQUE .....	23
3.4 LASER-INDUCED FLUORESCENCE.....	24
3.5 THE FUEL INDUCED GAMMA EFFECT .....	25
<b>4. DEVELOPING A SIMPLE, INEXPENSIVE TECHNIQUE.....</b>	<b>26</b>
<b>5. THE EXPERIMENTAL SETUP AND PROCEDURE.....</b>	<b>29</b>
5.1 SETUP.....	29
5.2 PROCEDURE.....	31
<b>6. DETAILED ANALYSIS OF THE FIGE MODEL .....</b>	<b>33</b>
6.1 INTRODUCTION TO THE MODEL.....	33
6.2 DEVELOPING AND CALIBRATING THE MODEL .....	33
6.2.1 <i>Effective Closing Angle</i> .....	38
6.2.2 <i>Mass Loss</i> .....	38
6.2.3 <i>Heat Transfer</i> .....	43
6.2.4 <i>Residuals</i> .....	48
6.2.5 <i>Putting it All Together</i> .....	49
6.3 FUEL INJECTION .....	52



6.3.1 Fuel Injection and the FIGE Process.....	52
6.3.2 Deriving the Evaporated Mass Equation .....	53
<b>7. RESULTS .....</b>	<b>58</b>
7.1 FIGE DEVELOPMENT .....	58
7.2 FIGE CALIBRATION .....	61
7.3 EVAPORATED FUEL MASS CALCULATION .....	64
<b>8. CONCLUSIONS AND RECOMMENDATIONS.....</b>	<b>68</b>
8.1 THE MOTORING CASE .....	69
8.2 THE FUEL INJECTION CASE .....	71
8.3 EVAPORATED FUEL MASS .....	72
<b>REFERENCES .....</b>	<b>76</b>
<b>APPENDIX A. MASS LOSS CALCULATION.....</b>	<b>77</b>
<b>APPENDIX B. RESIDUAL MASS CALCULATIONS .....</b>	<b>78</b>
<b>APPENDIX C. FIGE VISUAL BASIC CODE .....</b>	<b>81</b>

## TABLE OF FIGURES

FIGURE 2. 1 A PV DIAGRAM OF 10 KG OF AIR .....	7
FIGURE 2. 2 SCHEMATIC OF A PISTON-CYLINDER ASSEMBLY .....	15
FIGURE 2. 3 A FOUR-STROKE ENGINE PV DIAGRAM .....	16
FIGURE 2. 4 THE OTTO CYCLE .....	17
<del>FIGURE 6. 1 THE BASIC FIGE PROCESS FLOW DIAGRAM .....</del>	<del>37</del>
FIGURE 6. 2 MASS LOSS AS A FUNCTION OF IN-CYLINDER PRESSURE.....	42
FIGURE 6. 3 HEAT TRANSFER COEFFICIENT AS A FUNCTION OF CRANK ANGLE.....	47
FIGURE 6. 4 FIGE PROCESS FLOW INCLUDING LOSSES.....	51
FIGURE 7. 1 A PV DIAGRAM OF FIGE MOTORING DATA WITHOUT LOSSES.....	59
FIGURE 7. 2 PERCENT ERROR IN PRESSURE AS A FUNCTION OF CYLINDER VOLUME .....	60
FIGURE 7. 3 A PV DIAGRAM OF FIGE MOTORING DATA INCLUDING LOSSES .....	62
FIGURE 7. 4 PERCENT ERROR IN PRESSURE AS A FUNCTION OF CYLINDER VOLUME INCLUDING LOSSES .....	63
FIGURE 7. 5 A PV DIAGRAM OF FUEL INJECTED FIGE DATA .....	65
FIGURE 7. 6 PERCENT ERROR IN PRESSURE AS A FUNCTION OF CYLINDER VOLUME FOR FUEL INJECTION ...	66
FIGURE 7. 7 INJECTED FUEL EVAPORATION PROFILE .....	67

## ABSTRACT

The Fuel Induced Gamma Effect uses pressure data from a single-cylinder direct-injection engine and information about the specific heat ratio,  $\gamma$ , of the injected fuel to predict the evaporated fuel mass in the piston-cylinder assembly. Thermodynamic theory and ideal gas laws are used to calculate theoretical pressure within the cylinder and this pressure is then compared to the actual pressure measured in the engine. The difference in  $\gamma$  between the calculated and actual states of the fuel is then used to predict how much fuel has evaporated in the cylinder.

This simplistic approach also takes into account information about the residuals in the cylinder, mass loss from the system, and heat losses. Combining these factors with thermodynamic theory results in a very accurate model which can predict the evaporation profile of the injected fuel from the time of injection until ignition.

## 1. INTRODUCTION

The cost of fuel has risen significantly over the past few decades. This has driven the automotive industry to develop cheaper and more efficient internal combustion engines. One such development is the gasoline direct-injection internal combustion engine. This technology offers improved fuel economy and fewer emissions. Also, the power output of this type of engine will remain the same as or potentially improve over, current port fuel-injected engines. There are many aspects of this type of combustion technology that will need to be addressed in order for it to meet its full potential.

The concept of predicting the amount of fuel present at the time of ignition has been studied in recent years. A simple, inexpensive technique that is valid for most engine configurations has yet to be developed. The goal of this study is to use theoretical equations and a simple engine setup to develop an evaporation profile of the injected fuel from the time of injection until ignition occurs.

The Fuel Induced Gamma Effect technique, FIGE, was chosen for this study because of its simplicity and because other techniques only provided subjective results. The FIGE process can be used to determine the evaporation profile of fuel injected into any engine. It is not influenced by the injection spray pattern or engine configuration. Previous techniques used costly laser imaging equipment and were very difficult and time consuming to implement. The FIGE technique is simple because it can be used on any direct-injection engine equipped with a pressure transducer.

In the present work, pressure data from a single-cylinder direct-injection engine and information about the specific heat ratio of isooctane, the injected fuel, will be used to predict the evaporated fuel mass in the piston-cylinder assembly. Theory is used to

predict the in-cylinder pressure at every crank angle. The specific heat ratio is calculated at these conditions and compared to the calculated specific heat ratio based on the engine test results. The difference in these ratios is then used to calculate the mass of evaporated fuel present in the cylinder. These calculations can be performed on a crank angle by crank angle basis. The result is a graphical representation of the evaporation profile. The profile can then be used to predict when ignition should occur or the liquid to vapor ratio of the fuel at the time of ignition if ignition does occur. This information will lead to better, more efficient engines that produce fewer emissions.

## 2. THE THEORY AND HISTORY OF FUEL INJECTED INTERNAL COMBUSTION ENGINES

### *2.1 Thermodynamic Theory*

Internal combustion engines use the combustion of fuel to convert chemical energy into mechanical work output. To accomplish this, the chemical energy must first be converted to the internal energy of the gaseous medium. This internal energy, in turn, is converted to mechanical work output. The conversion in the first stage is dependent upon the type of fuel that is used and can be quantified using a bomb calorimeter to measure the heating value, or enthalpy of formation. Thermodynamic processes can be used to model the second stage; these processes will be explained in detail.

Furthermore, once a combustion cycle is modeled using thermodynamics, it can be compared to a real cycle. If the theoretical model accurately predicts real engine cycles, it can be used to optimize engine performance parameters. A theoretical model will be discussed to give a better understanding of the processes involved in the combustion cycle.

Parameters important to engine performance include air/fuel ratio, timing of fuel entering the cylinder, and ignition timing. Engines have used different systems to introduce fuel into the cylinder, including carburetors, port fuel injection, and direct fuel injection. The history of these systems will also be discussed later in this section.

#### 2.1.1 The First Law of Thermodynamics

A basic knowledge of thermodynamic theory is necessary to completely understand the combustion process. The First Law of Thermodynamics is a good starting

point for this material. The First Law states that the total change of energy within a system is equal to the net energy transferred to the system by heat transfer minus the net work done by the system. This can be written in equation form as

$$\Delta E = Q - W \quad (2-1)$$

where

$$\Delta E = \Delta KE + \Delta PE + \Delta U \quad (2-2)$$

and  $\Delta KE$  is the change in kinetic energy,  $\Delta PE$  is the change in potential energy,  $\Delta U$  is the change in internal energy,  $Q$  is heat transfer to the system, and  $W$  is the work done by the system.

The change in total energy of a system,  $\Delta E$ , is made up of three contributions, as shown above. The change in kinetic energy is associated with the motion of the system as a whole, relative to an external coordinate frame. The change in gravitational potential energy is associated with the position of the system as a whole in the earth's gravitational field. Internal energy is an extensive property of the system and includes all other energy changes (Moran and Shapiro, 1995).

### 2.1.2 Ideal Gases

Ideal gases are an integral part of the study of thermodynamics and thus play an important role in combustion engine theory. An ideal gas is a fictitious substance in the gaseous phase whose proportional dependence at constant volume of temperature on pressure holds for all pressures (Moran and Shapiro, 1995). The ideal gas equation of state relates these quantities:

$$pV = mRT \quad (2-3)$$

where

$$R = R_u / M \quad (2-4)$$

and  $R_u$  is the universal gas constant and  $M$  is the molecular weight of the substance.

“The ideal gas equation of state is obeyed approximately by a real gas whose pressure is not too large and whose temperature is not too low – that is, a dilute gas” (Moran and Shapiro, 1995). In the context of this paper, all gases being studied will be assumed to be ideal gases unless otherwise stated.

The ideal gas equation of state allows for the determination of one variable in terms of all others. Since most processes occur with a fixed mass of gas, knowing two of the remaining three will determine the third. By choosing pressure and volume as independent variables, the temperature can be determined. These states can be represented on a p-V diagram. Figure 2.1 shows a p-V diagram for air.

Four types of processes can be shown on a p-V diagram. A vertical line represents a constant volume process, which is called isochoric. Similarly, a horizontal line represents a constant pressure process, which is called isobaric. The curve represented by an isothermal process (constant temperature) depends on the equation of state of the system. An adiabatic process, as will be discussed later, is one in which there is no heat transfer to the system. The curve it produces is entirely dependent on the system.

Another important application of the ideal gas equation of state is for a constant mass system. For a constant mass system, the following relation applies

$$\frac{pV}{T} = C \quad (2-5)$$



where  $C$  is constant. This is useful in determining successive values of  $p$ ,  $V$ , or  $T$  in a process because

$$\frac{p_i V_i}{T_i} = \frac{p_f V_f}{T_f} \quad (2-6)$$

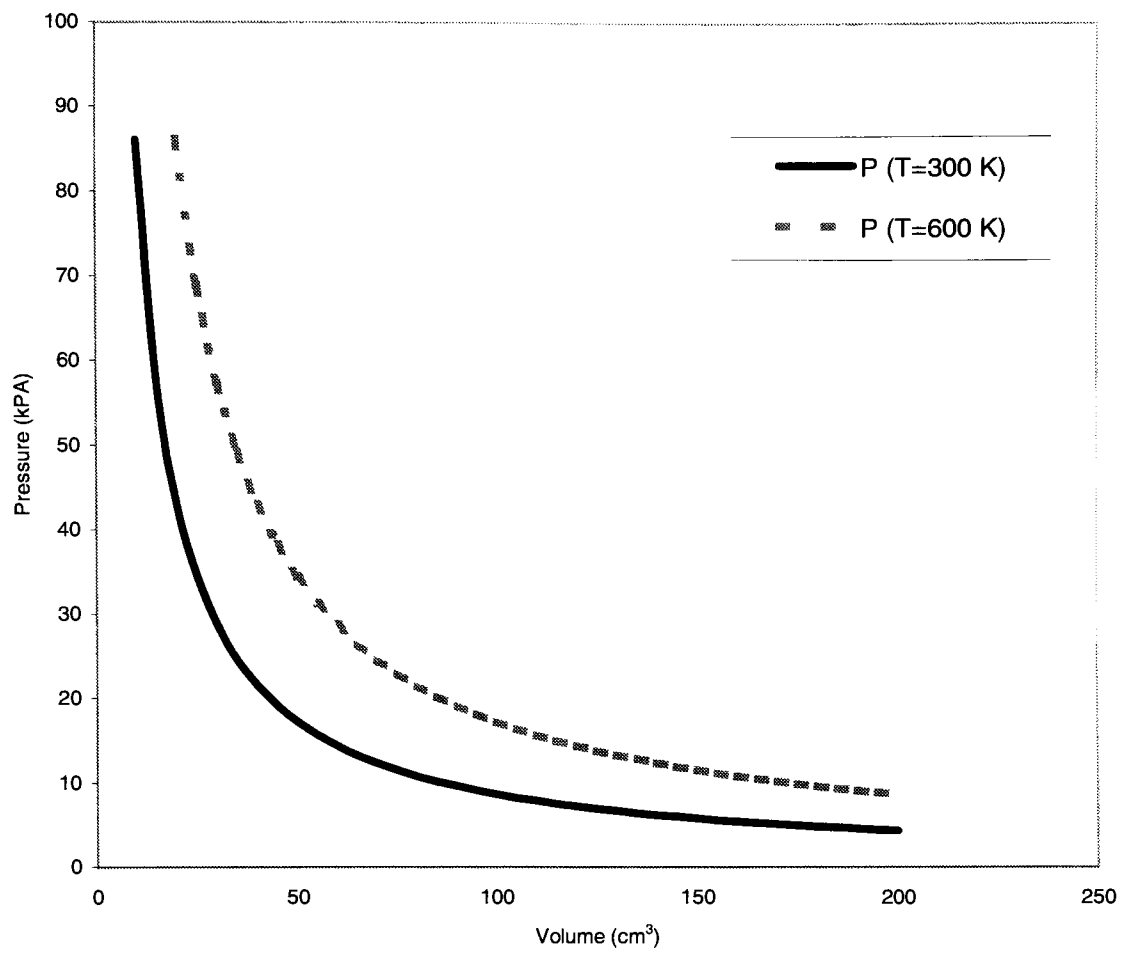


**Figure 2. 1 A pV Diagram of 10 kg of Air**

### 2.1.3 Heat Transfer

Heat transfer to and from a system can be calculated in several different ways. Those important to the content of this paper will be discussed here. Convection is described as being the energy transfer between a surface and a fluid moving over the surface (Incropera and Dewitt, 1996). The heat transfer rate is proportional to the difference in temperature between the surface,  $T_s$ , and the fluid,  $T_\infty$ , multiplied by the area,  $A_s$ . The proportionality constant is the convective heat transfer coefficient,  $h_T$ . Written in equation form, this is

$$Q = h_T A_s (T_s - T_\infty) \quad (2-7)$$

where  $Q$  is the heat transfer by convection between the surface and the fluid.

In this study, heat transfer by convection occurs between the cylinder and the air/fuel mixture in the combustion chamber. A second mode of heat transfer can be defined by a change in temperature of a substance due to the addition of heat to that substance. Before starting a discussion on this second mode of heat transfer, it is helpful to define several parameters.

The sum of specific internal energy and the product of pressure and specific volume is a quantity often required for thermodynamic calculations. This quantity,  $h$ , is defined as:

$$h = u + pv \quad (2-8)$$

and is called specific enthalpy. “The specific heat of a substance is the heat required to increase the temperature of 1 kg of the substance by 1 K” (Keller, Gettys, and Skove, 1993). The process by which a substance changes temperature will directly influence its specific heat. Two process-dependent specific heats are typically defined: specific heat at

constant pressure,  $c_p$ , and specific heat at constant volume,  $c_v$ . For ideal gases,  $c_p$  and  $c_v$  are defined as follows:

$$c_v = \frac{\partial u}{\partial T} \quad (2-9)$$

$$c_p = \frac{\partial h}{\partial T} \quad (2-10)$$

In addition,

$$c_p - c_v = R \quad (2-11)$$

The quantities  $c_p(T)$  and  $c_v(T)$  are functions of temperature; if the variation is small over the temperature range they can be assumed to be constant. The constant value can be calculated as follows:

$$c_v = \frac{\int_{T_i}^{T_f} c_v(T) dT}{T_f - T_i} \quad (2-12)$$

$$c_p = \frac{\int_{T_i}^{T_f} c_p(T) dT}{T_f - T_i} \quad (2-13)$$

(Moran and Shapiro, 1995).

The last quantity to be defined is the ratio of specific heats,  $\gamma$ .

$$\gamma = \frac{c_p}{c_v} \quad (2-14)$$

Another point worth noting in this section relates to multiple gases. When several gases are combined in an enclosed area, the properties of the mixture are a combination of the properties of the individual gases. In the case of pressure the total pressure is the

sum of the partial pressures of the individual gases. As with all other intensive properties, the specific heat is not a simple summation. The following formula applies:

$$z_t = \frac{\sum_i m_i z_i}{\sum_i m_i} \quad (2-15)$$

where  $z$  is the property in question, the subscript  $t$  is the combined value for that property and the subscript  $i$  is the property for each individual gas.

When heat is transferred to a substance and causes a temperature change, it can be defined using specific heats. If heat is added during a constant pressure process, the amount of heat is defined by

$$Q = mc_p \Delta T . \quad (2-16)$$

For a constant volume process the definition is

$$Q = mc_v \Delta T . \quad (2-17)$$

Some real processes occur so quickly that a negligible amount of heat is added. This type of process is called adiabatic. The compression stroke of an internal combustion engine can be approximated as being adiabatic. Keller, Gettys, and Skove (1993) have shown that for an adiabatic process using an ideal gas

$$pV^\gamma = K \quad (2-18)$$

where  $K$  is constant.

#### 2.1.4 Work

“Work is energy transferred between a system and its environment by means independent of the temperature difference between them” (Moran and Shapiro, 1995). In

this study, the work done will be caused by the expansion of the working gas in a piston cylinder assembly. In this case work is defined as

$$W = \int_{v_1}^{v_2} p dV \quad (2-19)$$

The work done by a process according to this equation is the area under the curve on a p-V diagram. For an isobaric process, the work will be equal to the product of pressure and change in volume. The work done by an ideal gas during an adiabatic process is

$$W_Q = \frac{P_i V_i}{\gamma - 1} \left[ 1 - \left( \frac{V_i}{V_f} \right)^{(\gamma-1)} \right] \quad (2-20)$$

The subscripts  $i$  and  $f$  denote the initial and final states, respectively.

Work can be either positive or negative. During a volume expansion process work will always be positive. For a compression process the opposite is true. As will be seen more clearly in later sections the work done during a complete cycle is the area between the expansion and compression curves on a p-V diagram.

### 2.1.5 The Otto Cycle

The material presented so far in this paper has been provided to aid in developing the criteria for judging the performance of an internal combustion engine. To further this development the Air-Standard Otto Cycle will be presented. The Otto cycle is a theoretical model used as a basis for comparison to a spark ignition engine.

A reciprocating internal combustion engine is the system modeled. Figure 2.2 is a schematic of a reciprocating internal combustion engine. It depicts a piston moving in a

cylinder fitted with valves and a spark plug. Several important terms are labeled on the schematic. The bore is the cylinder diameter. The stroke is the distance the piston travels from bottom dead center (maximum cylinder volume) to top dead center (minimum cylinder volume). The minimum cylinder volume at top dead center (TDC) is called the clearance volume. As the piston moves from bottom dead center (BDC) to TDC it sweeps through a volume which is known as the displacement volume. The compression ratio of the engine is the volume at BDC divided by the volume at TDC. The crank mechanism converts the reciprocating motion of the piston into rotary motion, which is the useable work output.

The internal combustion engines being modeled operate with four distinct strokes during two complete revolutions of the crankshaft. Some engines run on a two-stroke process, but these will not be discussed. Figure 2.3 shows a p-V diagram for a typical four-stroke process. The start of the cycle begins with the piston at TDC. The intake valve opens and the piston moves downward, drawing in a combustible charge of the air/fuel mixture; this is the intake or *induction stroke*. With both valves closed the piston moves upward compressing the charge, in the *compression stroke*. This also raises the temperature. The combustion process begins by firing the spark plug. The combustion creates a high-temperature, high-pressure gas mixture, which expands and forces the piston downward. This is defined as the *power stroke*. The piston moves back to TDC with the exhaust valve open, purging the burnt gases from the cylinder. This is known as the *exhaust stroke*.

The Air-Standard Otto Cycle attempts to model the compression and power strokes of the spark-ignition internal combustion engine. In order to model this cycle

accurately, an instantaneous heat addition process occurring at TDC replaces the combustion process. The Otto cycle is shown in Figure 2.4 on a p-V diagram. The four processes shown are as follows:

- 1-2    isentropic compression of air through the compression ratio
- 2-3    heat addition at constant volume,  $Q_{23}$
- 3-4    isentropic expansion of air to original volume
- 4-1    heat rejection at constant volume,  $Q_{41}$ .

Efficiency is defined as the work output divided by the heat addition during the cycle. For the Otto cycle the efficiency,  $\eta_{Otto}$ , is

$$\eta_{Otto} = \frac{W}{Q_{23}} \quad (2-21)$$

From the First Law,  $\Delta W = \Delta Q$ , neglecting changes in kinetic and potential energy.

Therefore  $W = Q_{23} - Q_{41}$ , so

$$\eta_{Otto} = 1 - \frac{Q_{41}}{Q_{23}} \quad (2-22)$$

Since air is being considered as an ideal gas with constant specific heats,

$$\begin{aligned} Q_{23} &= mc_v(T_3 - T_2) \\ Q_{41} &= mc_v(T_4 - T_1) \end{aligned} \quad (2-23)$$

For the two isentropic processes,  $TV^{\gamma-1}$  is constant; therefore

$$\frac{T_2}{T_1} = \frac{T_3}{T_4} = r_v^{\gamma-1} \quad (2-24)$$

and

$$\eta_{Otto} = 1 - \frac{1}{r_v^{\gamma-1}} \quad (2-25)$$



By specifying the compression ratio and using a constant  $\gamma$ , the efficiency of a real engine can be approximated.

The Otto Cycle has been presented to aid in the understanding of the processes used to model an internal combustion engine. The model helps to simplify the study of internal combustion engines, but at times it may not accurately predict the real processes.

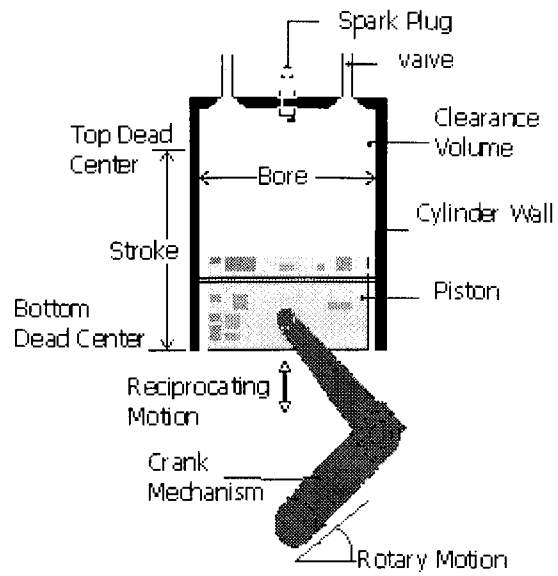


**Figure 2. 2 Schematic of a Piston-Cylinder Assembly**

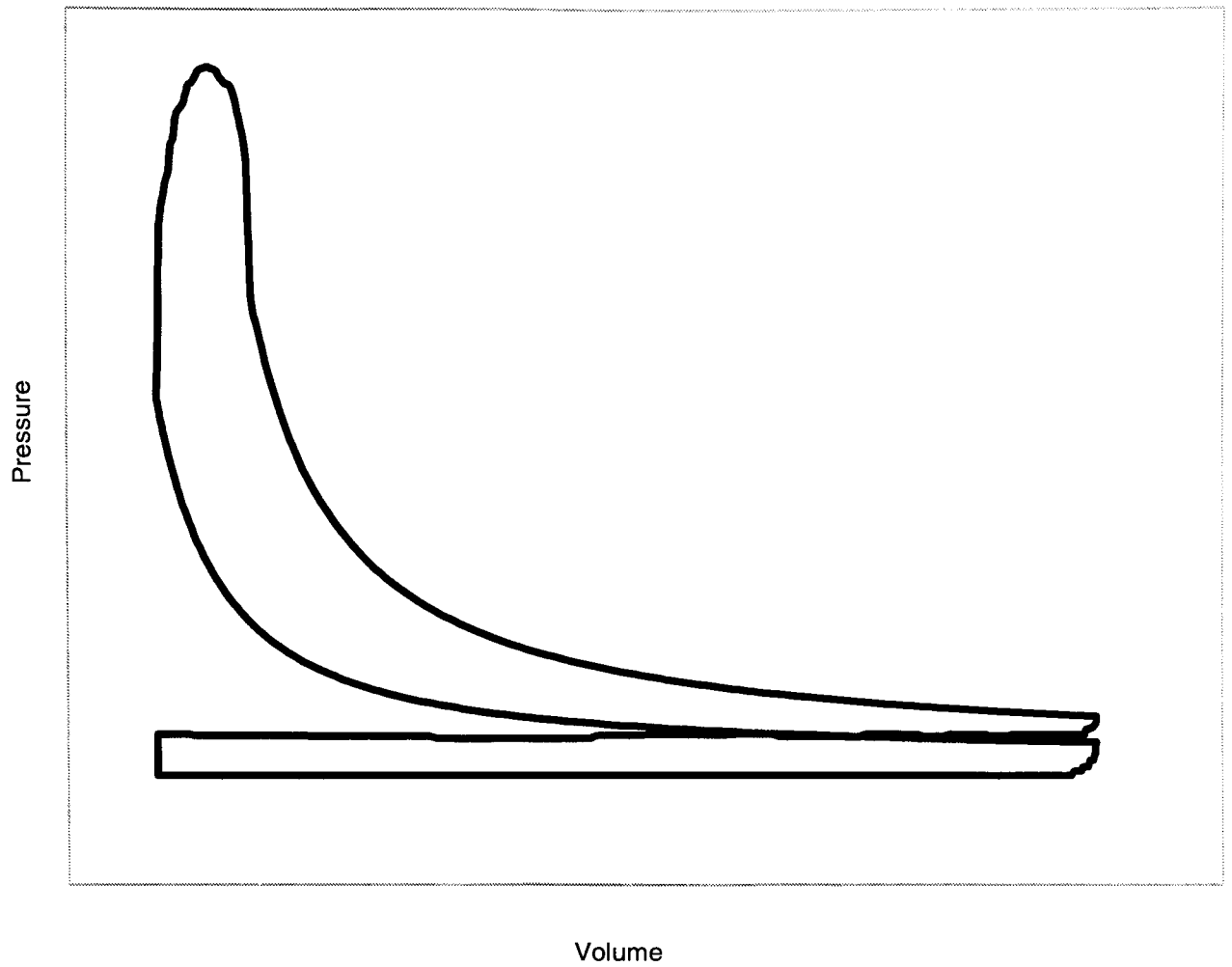


**Figure 2. 3 A Four-Stroke Engine pV Diagram**

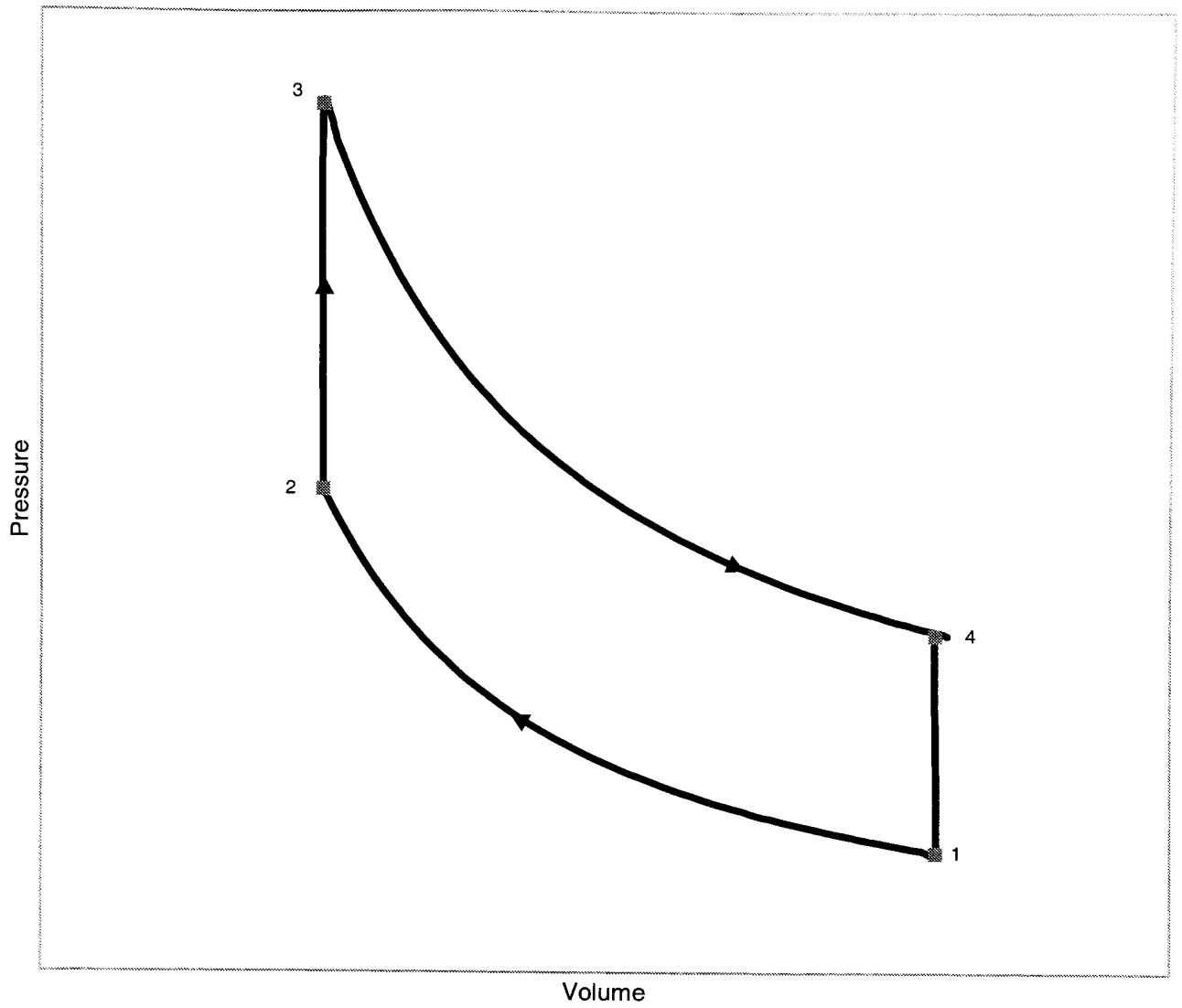


**Figure 2. 4 The Otto Cycle**

## *2.2 Fuel Injection Devices*

Spark-ignition internal combustion engines create power and torque. Introducing different amounts of a combustible mixture into the cylinders of the engine can regulate these quantities. A fuel injector or a combination of a carburetor and throttle valve is used to control this mixture.

Complete combustion requires a stoichiometric mixture of fuel and air. This means that an exact air to fuel ratio is required to obtain complete combustion of both products. There are different types of devices that aid in obtaining the proper mixture. These are the carburetor and the fuel injector. The fuel injector injects fuel either directly into the cylinder (direct injection) or into an inlet manifold (indirect or port fuel injection).

Carburation and port fuel injection will be briefly discussed to give general background information. The details of direct injection will also be discussed to further the understanding of the most difficult and most important aspect of this study.

### **2.2.1 Carburation**

The carburetor was one of the earliest devices used to introduce fuel into the cylinder. Initially it was a mechanical device, but has evolved and changed in design since its introduction.

As stated by Newton, Garrett, and Steeds (1996), the carburetor is essentially comprised of an air intake (also called an air horn) through which air passes into a venturi. The venturi is a tube in which there is a throat of a streamline section. The

velocity of the air flowing to the narrowest section increases; as the cross-section increases the velocity decreases. Due to the Bernoulli effect, the increased velocity causes a decrease in pressure. Fuel jets subjected to this lower pressure supply fuel to the engine. This is dependent upon the rate of airflow and the extent of the decrease in pressure. The throttle valve again controls these quantities.

There are some disadvantages to using carburetors. Carburetors rely on pressure differences, yet atmospheric pressure is not a constant quantity. Any variation will cause differing supplies of fuels for similar throttle and load conditions. Another disadvantage is that multiple carburetors are installed in order to optimize aerodynamic performance. Multiple carburetor installations will improve aerodynamic performance in the inlet manifold, but the carburetors then have to be balanced. Each will have to provide the same flow and mixture strength. Another problem according to Stone is, “it is quite usual for carburetors to give  $\pm 5$  per cent variation in mixture strength between cylinders, even for steady-state operation” (1992).

### 2.2.2 Port Fuel Injection

Fuel injectors were designed to optimize the performance of internal combustion engines. The pressure drop in the carburetor decreases power output and the volumetric efficiency of the engine. The original injector design was an entirely mechanical device with complex two-dimensional cams. Electronic circuits have replaced these.

There are two types of port fuel injection systems: single- and multi-point injection. The single-point injection is a cheaper alternative because only one injector is

used to inject fuel into the manifold. This, though, can lead to lower power output than the multi-point injection system. The multi-point injection system is more costly because it typically has one injector per engine cylinder, but these multiple injectors make it more efficient. Although the two types are quite different, the operating principle is very much the same. The differential pressure across the injector controls the fuel flow rate through it. The fuel is sprayed into the inlet manifold, where it can then be introduced into the cylinder during the induction process.

There are many benefits to port fuel injection over carburation. These are discussed by Newton, Garrett, and Steeds (1996) and include elimination of the venturi and throttle body heating, reduction of adverse effects of fuel movement in the float chamber, lower fuel consumption, higher torque, and increased power output. While using a carburetor, fuel may “stick” to the walls of the combustion chamber; this is called wall wetting. This fuel will not evaporate as quickly causing incomplete combustion, which causes high levels of emissions. For port fuel injection wall wetting is less prevalent. In port fuel injection fuel enrichment at start up is not needed, this too reduces emissions.

### 2.2.3 Direct Injection

Many automobile makers are looking into developing gasoline direct injection engines to reduce engine emissions, to improve engine efficiency, and to increase power output. This technique uses an injection system to inject fuel directly into the combustion chamber. The injection occurs at high pressures during the compression stroke of the

engine. This high-pressure injection results in rapid vaporization and smaller fuel droplet size. These two factors improve the combustion process, allowing for more complete combustion; therefore power output is increased and emissions are decreased.

Although direct injection has been readily available in diesel engines for many years, the concept of direct injection in gasoline engines is fairly new and has only been studied in depth for a short period of time. The leaders of the automotive industry have not yet standardized the direct injection process; there are many techniques employed to accomplish this type of injection. The electronic injector can be mounted in different locations depending on the process to be used. Also, the injection timing can vary depending on the process and the loads on the engine.

There are many advantages to direct injection. According to Fan, et al., these include “higher thermal efficiency, higher volumetric efficiency, lower fuel consumption, better driveability, and better cold start performance” (1999). The disadvantage of a direct injection system is that if the process is not performed correctly, hydrocarbon emissions will increase.

In summary, it has been shown that the benefits to fuel injection are much greater than carburation. The process of introducing fuel into the cylinder has been changed and modified throughout its history. From the early inception of the carburetor to the multi-point injection system and now to direct injection, the fuel system has developed greatly. New technology has been and will continually need to be developed to maintain and improve the quality and performance of the spark ignition engine.



### 3. STATE-OF-THE-ART FUEL QUALITY MEASUREMENT TECHNIQUES

Various studies have been performed to measure fuel spray characteristics for a direct injection spark ignition engine. These studies determined the fuel quality at the time of ignition. Fuel quality is the amount of fuel vaporized and mixed with air before ignition. The quality at ignition is a major factor influencing engine design. Varying this one parameter can lower engine emissions, improve fuel economy, and increase power output.

The state-of-the-art techniques used to measure fuel quality will be examined in this section. The techniques include vapor probe measurements, several laser techniques, and a technique that uses combustion chamber pressure measurements. Although these techniques are very useful, they will only be discussed in minor detail in order to give a concise background for this study.

#### *3.1 Fiber Optic Spark Plug Probe*

Alger, et al. (1999) used a fiber optic spark plug probe to measure vapor concentration near the spark plug. The probe consisted of two chalcogenide optical fibers, one used as a light source input, the other as an output. These fibers were fitted into a stainless steel tube that projected into the combustion chamber in place of the spark plug. Inside the combustion chamber the tube was fitted with a mirror. The sides of the tube were machined away to allow the fuel vapor to flow freely through the device.

A light source was modulated using a signal chopper to produce a square wave pattern. The signal passed through the input fiber and was reflected from the mirror onto

the output fiber. The light that reflected onto the second fiber was less intense than that coming from the first fiber because some of the radiation from the light was absorbed by the fuel vapor in the gap. This change could then be measured and correlated to vapor concentration.

### *3.2 The Optical Engine*

The majority of techniques that used a laser for measurement of the fuel quality at ignition also used an optical engine. These engines had some portion removed and replaced with a quartz window. In different studies, depending on the manufacturer, the quartz was the cylinder liner or in the combustion chamber head. The design of each device was also dependent upon the type of experiment performed.

According to C. William Robinson, these devices have been around since the 1970's at the Sandia National Laboratory. "The top of the combustion chamber was covered with a window made of quartz or sapphire. This large window exposed the entire combustion chamber"(1996). The design also included windows in the side of the cylinder to provide access for the laser beams. This was, and still is, the typical setup for the optical engine used in combustion research.

### *3.3 The Argon Ion Laser Technique*

In 1997 a single cylinder Ricardo Hydra optical engine was used at the University of Wisconsin-Madison to evaluate in-cylinder spray characteristics. This engine was very similar to the optical engine described above. Scott Parrish and Patrick Farrell

(1997) used an argon ion laser and several cylindrical lenses to create a laser sheet within the combustion chamber. The different lenses were used to orient the sheet through the windows in either a horizontal or vertical fashion.

With the laser in place, Parrish and Farrell (1997) could take snapshots of the injection spray using a sophisticated imaging system. These images were used to study the spray characteristics. The results of the study centered on the in-cylinder spray distribution and in-cylinder gas flow. They showed that although a symmetric, hollow, cone shaped spray would be optimal, the spray tended to be more asymmetric due to the high pressures and high in-cylinder fuel flow velocities.

### *3.4 Laser-Induced Fluorescence*

A study performed by Wolfgang Ipp, et al (1999) used laser-induced (exciplex) fluorescence, or LIEF. “By means of LIEF measurements the liquid fuel phase and the fuel vapor were simultaneously acquired onto two separate images, so that the influence of ambient conditions on the fuel vapor phase and spray evaporation was visualized”. This experimental setup was similar to, yet more complex than, the one used by Parrish and Farrell. A laser was used to form a sheet, which caused the fluorescence of the fuel. The complexity came in the form of choosing the correct fuel to cause the fluorescence of the fuel in both the liquid and vapor phases. In this study the non-fluorescing base fuel, isooctane doped with benzene and triethylamine, was used.

The results showed that the vapor phase followed the liquid spray throughout the injection process. The study also showed that by varying the injection temperature the spray could be compacted. An increase in temperature of both the injector body and the

fuel gave a visible reduction of large fuel drops. Although this technique was not 100% effective in separating the liquid and vapor phases, it was sufficient for the evaluation of the spray characteristics.

### *3.5 The Fuel Induced Gamma Effect*

The final technique to be discussed uses simple pressure transducers instead of high-tech measuring devices. The fuel induced gamma effect (FIGE) uses the pressure difference between the fueled case and the motored case without injection. “The technique relies on the significant difference in the ratio of specific heats, or gamma, of fuel from air or residual gases” (Witze, 1999). Witze also established a parameter to measure the change in pressure due to the vapor-phase fuel:

$$FIGE = \frac{P_{unfueled} - P_{fueled}}{P_{unfueled}} \times 100 \quad (3-1)$$

By collecting pressure data before and after injection for different types of injection, Witze quantified the amount of vapor-phase fuel. He utilized a plot of the FIGE parameter for different injection timings and opened- and closed-valve injection to find the optimum injection timing. The optimum occurred where FIGE was at a maximum, which was the point where the fuel vaporized the most.

These techniques are all very useful in measuring fuel quality. Some are very expensive and require expertise in the field. Others are simple and can be done on standard engine test setups with minor adjustments. To date, these are the most widely used and most technically advanced techniques in the automotive industry for measuring fuel quality at injection.

#### 4. DEVELOPING A SIMPLE, INEXPENSIVE TECHNIQUE

Many techniques that attempt to measure the amount of vapor phase fuel present in the combustion chamber at the time of ignition are costly and difficult to implement. The goal of this study is to research and develop a simple, inexpensive, theoretical technique that will provide adequate results. This technique will be based on the FIGE technique developed by Witze. The specific heat ratio of air and fuel will be used to determine the amount of vapor phase fuel present during the compression stroke and this information will be used to predict the ignition timing.

As the difficulty of a technique increases, the cost of implementing that technique tends to increase. A simple technique will use existing, inexpensive technologies to collect data. This will allow engineers and scientists more time to verify the accuracy of the data and to find a solution to the problem. The alternative would be time spent on developing new tools and equipment to collect data.

The goal is to provide adequate results, but what does this mean? What are adequate results? In order to define the adequacy of the results, it is necessary to know what the results will be used for. The results of this study will be used to optimize the combustion process in a gasoline direct-injection spark-ignition engine. This optimization will improve fuel economy and increase power output while lowering the emissions from the engine.

Injection timing will aid in the improvement and optimization of these three parameters. Therefore, adequate results will determine the injection timing. The model should be able to predict within a few crank angle degrees when injection should occur.

Minor adjustments could be made on a test engine to more closely optimize the parameters.

A modified Fuel Induced Gamma Effect technique will be introduced in this study. There are many advantages of using this technique over the techniques previously studied. Two important benefits are cost and accuracy of the results. For many of the earlier studies, it was very expensive to develop and use the techniques. The cost of a technique depends on many things, including equipment costs, knowledge base, and labor costs.

Most of the earlier techniques used a costly laser for measurements. The laser also required the research and development of the proper lenses to focus the laser beam into the necessary pattern. Then, state-of-the-art-imaging equipment was used to photograph an image of the spray pattern; this too was very expensive. The only way to take the necessary photographs was to design, build, and test an optical engine. It is evident this that the cost of implementing these techniques was very high.

The accuracy of the previous techniques was adequate, although most of the studies showed results that tended to be subjective. The spark plug probe only gave results in the area of the spark plug. All of the laser techniques gave a two-dimensional image of a three-dimensional spray pattern. These 2D patterns were then interpreted to find 3D results. In several of the experiments the spray pattern was imaged using three orthogonal views to improve on the accuracy of the results, although the requirement of laser lighting only allowed one view to be photographed at a time. This means that the accuracy of the results were highly dependent upon the repeatability of the injected fuel spray and the same testing environment conditions.

There are several uses for a simple, inexpensive technique to measure vapor phase fuel in a direct-injection spark-ignition engine. Such a technique will provide the means to quickly and easily develop new engines and to verify results from previous studies. This will greatly increase the knowledge base of the automotive industry.

The theoretical nature of the modified FIGE technique will allow the input of different variables in such a way that different engines can be tested before ever being built. If the results were promising, a model could be built to test the accuracy of the design and improvements could be made from that point. This will be more cost effective than designing and building an engine and then testing it to see if it will work.

By using the engine setups that were developed for the other techniques, the results of a FIGE model can be verified. The older techniques may have given perfect results, but there was no way of knowing how good these results were. Another verification method will provide a basis for comparing results.

As stated earlier, the results found in this study will add to the knowledge base of the automotive industry. As this knowledge base grows, the products that are made will be increasingly better. They will use less fuel, provide more power, and be less harmful to the environment.

## 5. THE EXPERIMENTAL SETUP AND PROCEDURE

This study required experimentation and data acquisition for two important reasons: to create a pressure-volume model of an engine cylinder cycle and to evaluate the final results of this model. The data collected had to consist of values pertinent to the model, most importantly pressure as a function of cylinder volume. It was also necessary to collect several extra, but necessary, data including initial temperature of the system and the mass of the exhaust gases. All of the data for this study was collected at the Customer Solutions Center at Technical Center Rochester, a division of Delphi Automotive Systems. The team at Delphi used well-known processes and data collection techniques for the study. This allowed them the ability to use existing test setups with only minor changes. A detailed explanation of the setup and procedure follows.

### *5.1 Setup*

All of the experiments necessary to conduct this study were performed on a Ricardo Single Cylinder Research Engine. This engine had a top entry reverse tumble piston impingement Direct Injection Gasoline (DI-G) combustion chamber. The valve train consisted of two intake valves and two exhaust valves with overhead direct acting mechanical buckets. The Delphi Micro DI-G injector, which required 10 MPa of fuel pressure, was located on the side of the combustion chamber. The engine displacement was 0.3225 L. The dimensions of the engine's cylinder were 74 mm and 75 mm for the bore and stroke, respectively. Several other relevant engine constants are shown in Table 5.1. These constants will be further explained throughout the remainder of this study.



Max Cyl. Surface Temp (K)	533
Min Cyl. Surface Temp (K)	483
Engine Speed (RPM)	1300
Cylinder Bore (mm)	74
Piston Head Area (cm <sup>2</sup> )	43
Clearance Area (cm <sup>2</sup> )	54.97
Clearance Volume (cm <sup>3</sup> )	31.12
Total Volume (cm <sup>3</sup> )	356.26
Atmospheric Pressure (kPa)	101
Injected Fuel	Isooctane

Table 5.1 Engine Constants

The engine was tested in Delphi's test cell #7, which had the necessary equipment for data acquisition. A Cussins Technology engine dynamometer with coolant and oil temperature control was used as the test bed. The combustion air supply was thermodynamically controlled. A 30° to 122°F temperature range could be achieved. The humidity could be controlled between -2° and 120°F dewpoint. The pressure was controlled from 70 to 110 kPa (absolute) with a flow rate of up to 100 CFM. A 5-gallon Haskel Cart that could be pressurized from 0 to 12 MPa (absolute) supplied the fuel.

Emissions of N<sub>2</sub>, NO<sub>x</sub>, CO, CO<sub>2</sub>, and O<sub>2</sub> were measured using the Peirburg technique. This technique takes the entire exhaust gas from the engine and dilutes it with air to prevent chemical reactions and condensation in the sample. Samples that correlate to various driving conditions and periods of time are taken and collected in bags. An exhaust emission bench is used to combine the sample analysis data and the volume of the sample. The resulting calculation gives the mass of each component emitted from the test engine.

An inline high pressure Micro Motion sensor measured the fuel pressure. A cylinder head mounted Kistler 6121 pressure transducer was used to measure the cylinder

pressure. DSP ACAP version 5.0 was used for high-speed data acquisition and combustion chamber analysis. Microsoft Excel 97 and Microsoft Visual Basic were used to retrieve and analyze the data.

Several factors remained constant throughout the testing process. The engine speed was set to 1300 rpm. It is important to note that the engine speed varied slightly throughout the testing cycle, although the variation was never greater than 0.5%. The mean speed remained constant at 1300 rpm, and was considered constant throughout this study. A load of 330 kPa (net mean effective pressure) was placed on the engine. The coolant temperature was kept at a constant 90°C with the inlet air temperature at 25°C. Each data set consisted of 10 engine cycles in which cylinder pressure data was taken on a crank angle basis. As part of the data set, the cylinder volume corresponding to the crank angle was calculated.

## *5.2 Procedure*

Early injection timing was studied because the evaporation of the fuel would be more evident at this stage of injection. As a result of lower temperatures at the beginning of compression, evaporation would occur more slowly. The test procedure was to start the engine and motor it while injecting fuel until a steady state was reached. At that point, fuel injection continued and ten four-stroke cycles of data were collected. A single injection occurred during each of these cycles. The injector was then turned off; motoring continued and a second data set consisting of ten cycles was collected. The two data sets were later used to help build the FIGE model.

There were two reasons for collecting data in this fashion. The first was to minimize the initial value errors between the two data sets. At steady state, the initial cylinder temperature for both the motoring case and injection case would be nearly identical, reducing any effects of mismatched data. Also, the air in the cylinder after injection contained residuals from combustion. Any difference in pressure data between the two data sets caused by these residual gases was minimized. The second reason for collecting data in this manner was to minimize the effects of false pressure readings. The pressure at every point was calculated by eliminating the highest and lowest pressure values of the ten cycles for that point and then taking the average of the remaining eight readings. This provided a “smoothed” data set, which could be more accurately modeled. This smoothing would also take into account the fact that during motoring, residuals would be cleaned from the system and the mixture would tend to behave like pure air.

Isooctane acts like an ideal gas in the vapor phase, it was readily available in the test cell, and its gamma data is well documented; therefore it was the fuel injected into the cylinder. Typically, 15mg of fuel was injected into the cylinder during each cycle.

## 6. DETAILED ANALYSIS OF THE FIGE MODEL

### *6.1 Introduction to the Model*

As stated in Section 4, the goal of this study is to find an inexpensive technique to obtain the mass of fuel that has evaporated in an engine cylinder prior to combustion. In order to accomplish this task, the Fuel Induced Gamma Effect (FIGE) model was created. This section will completely describe the FIGE model.

The FIGE model uses the specific heat ratio of the air and gaseous fuel (isooctane in this study) to extract the mass of fuel from pressure and volume data. Theoretical equations for ideal gases are used to model the pressure with respect to cylinder volume. By comparing the expected pressure values from the model to the actual values from the experiments, a difference is found. Taking into account several other factors that cause pressure variations, the mass of the fuel can be correlated to the differences in pressure.

The creation of the model took several steps. First, the model had to be calibrated to be sure that it performed accurately. To refine the model, factors such as mass loss, heat transfer, and residuals in the cylinder were added. Then fuel calculations were performed to complete the model. Finally, the model was tested for accuracy. These steps will be explained in detail throughout the remainder of this section.

### *6.2 Developing and Calibrating the Model*

The FIGE model is based upon equations 2-5 and 2-18. These equations relate the pressure, volume, and temperature of the air/fuel vapor mixtures to the ratio of specific heats at these conditions. To begin the model, the volume data for the

compression stroke of the cylinder was needed. These values were taken from the data set provided by Delphi and remained constant throughout the entire study. Two other data points were needed to begin modeling; these were the initial pressure and the initial temperature of the gases in the cylinder. The initial pressure,  $P_i$ , was extracted from the data set at the corresponding volume,  $V_i$ .

The initial temperature,  $T_i$ , was more difficult to measure. This was because there was no convenient way to place a thermocouple inside the cylinder. The air in the cylinder at bottom dead center comes primarily from the intake stroke. The intake air comes directly from the atmosphere, or in this case the test cell. Therefore the initial temperature was assumed to be the regulated test cell temperature.

A graphical representation of the pressure with respect to volume was necessary to create the model and correlate the data. A graphical model was created by calculating the pressure at incremental volume steps (or at every crank angle). For each step there was an initial value, or the current value of the parameter, as well as a final value, or the value at the next step. These will be denoted by the subscripts  $i$  and  $f$ , respectively.

The first step in calculating the pressure at point 2, the final volume, was to assume a final temperature,  $T_f$ . For convenience, the final temperature was assumed to be equal to the initial temperature,  $T_i$ . Only motoring data was used; for the development and calibration of the model therefore there was no fuel in the cylinder. Knowing both  $T_i$  and  $T_f$ , an average specific heat ratio,  $\gamma_{ave}$ , could be calculated using equations 2-12 through 2-14, where

$$c_p(T) = 7.929 \times 10^{-14} T^4 - 5.490 \times 10^{-10} T^3 + 9.453 \times 10^{-7} T^2 - 0.0004T + 1.048 \quad (6-1)$$

$$c_v(T) = 7.929 \times 10^{-14} T^4 - 5.490 \times 10^{-10} T^3 + 9.453 \times 10^{-7} T^2 - 0.0004T + 0.761 \quad (6-2)$$

These equations for specific heat of air were derived from Table A.4 Thermophysical Properties of Gases at Atmospheric Pressure (Incropera and Dewitt, 1996) using the “LINEST” function in Excel. Then, by rearranging 2-18, a final pressure,  $P_f$  could be calculated as follows:

$$P_i V_i^\gamma = P_f V_f^\gamma \quad (6-3a)$$

$$P_f = P_i \left( \frac{V_i}{V_f} \right)^{\gamma_{ave}} \quad (6-3b)$$

where  $\gamma_{ave}$  is the value calculated from equation 2-14.

This  $P_f$  was calculated using an assumed value of  $T_f$ , so there was uncertainty in the final value. A verification of  $T_f$  was needed. This was done using equation 2-6.

Solving for  $T_f$ ,

$$T_f = \frac{P_f V_f T_i}{P_i V_i} \quad (6-4)$$

However, this calculated  $T_f$  may not equal the temperature assumed at the beginning of the process. Now,  $T_f$  replaced the assumed final temperature and the process was repeated until the assumed final temperature and the calculated final temperature were equal. This is the FIGE process. Figure 6.1 shows the flow of this process. The FIGE process was continued for each crank angle until the piston reached TDC.

This process is the basis for the model. Next, the model had to be calibrated to match the data collected at Delphi. The calibration could only be done by matching the data on a point by point basis to see if the overall fit was sufficient. The means of doing this was to find the percent deviation from the actual value of each calculated pressure.

$$\%E = \left| \frac{P_{calc} - P_{data}}{P_{data}} \right| \times 100 \quad (6-5)$$

where  $P_{calc}$  is the calculated pressure and  $P_{data}$  is the data pressure. The standard deviation of the percent deviation was calculated using Excel's "STDEV" function. By adding various parameters to the model, the standard deviation was minimized, resulting in the best-fit model. The following sections will detail these parameters and how they were added to the model.

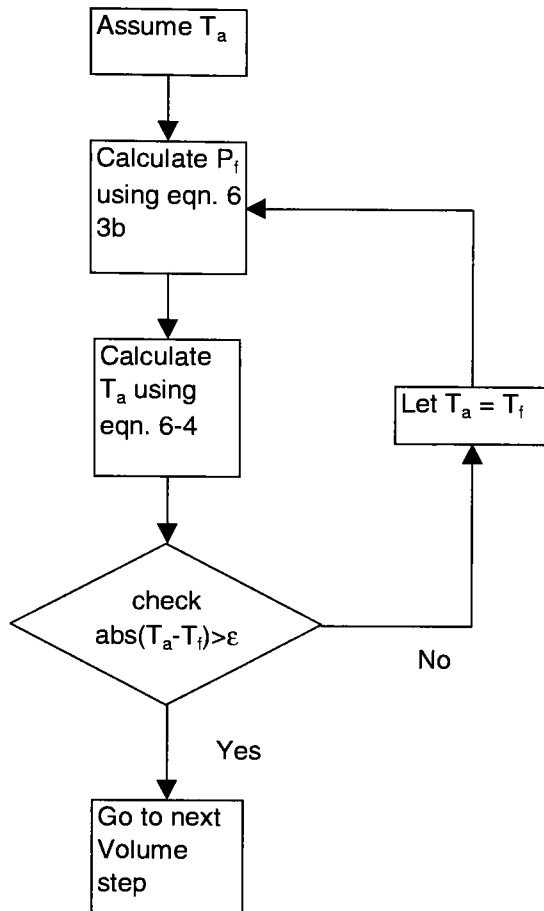


**Figure 6. 1 The Basic FIGE Process Flow Diagram**



### 6.2.1 Effective Closing Angle

An engine cycle is a complex cycle to model; many factors have to be considered to be sure that the model resembles the physical cycle. One such factor that is important is the crank angle at which the intake valve closes, which is the *effective closing angle*. This is important because compression does not begin until this valve is fully closed.

As the piston comes to the BDC position at the end of the intake stroke, the intake valve should close. In reality this does not occur because of timing delays, pressure in the system, and various other factors. Instead, the valve closes shortly after BDC and compression begins.

In order for the model to perform properly, the pressure at the effective closing angle had to be used as the initial pressure. This crank angle was used for the starting point of the model. The effective closing angle had to be determined or calculated. This turned out to be a very simple task. Using the data that had been collected it, was seen that after BDC the pressure remains fairly constant for a number of crank angle degrees. Beyond this point the pressure began to increase. Although not exact, the effective closing angle could be assumed to be at the end of this constant pressure process. The effective closing angle is not a constant value and had to be determined for each subsequent data set.

### 6.2.2 Mass Loss

A realization was made very early in this study that there are no ideal or perfect systems, especially engine systems. There will be leaks in the piston cylinder assembly

in which quantities of air and fuel will be lost through the ring seals around the piston.

There are two ways to approach calculating the resulting mass loss. The first is to use the pressure differentials between the combustion chamber and atmospheric pressure conditions along with information about the cross-sectional area through which the air and fuel will leak. The second is to derive empirical results from the collected data. The second method, the simpler of the two, was chosen because it would give adequate results for this study. The first method could be developed into a full-scale study and would be difficult to pursue.

Several factors had to be considered in order to derive an equation for mass loss. The first was a conceptual idea of how the equation should behave. The initial thought was that as the internal pressure increased, while the atmospheric pressure remained constant, the pressure differential increased and the mass loss would increase. However, this was not accurate and actually the opposite was true, as will be shown.

As the pressure increased, the internal temperature also increased. The result of this increased temperature was an expansion of the ring seals. Combining this expansion with the increased pressure, the area through which gases could escape, and thus the mass loss, decreased. As a result, as the pressure increased the mass loss decreased to a point where there was essentially no mass loss.

The problem then was to determine the mass loss as a function of pressure. This was derived using both the collected data and a variation of the FIGE process as shown above. For each pressure data point collected a corresponding temperature was calculated using equation 6-4:

$$T_f = \frac{P_f V_f T_i}{P_i V_i} \quad (6-4)$$

Using this and the initial temperature,  $\gamma_{air}$  was calculated. Then equation 6-3 was used to calculate  $P_{calc}$ . With equation 2-3 and the final values,  $m_{calc}$  and  $m_{data}$  could be calculated using  $P_{calc}$  and  $P_f$ , respectively. By subtracting the data mass from that of the calculated, the mass loss was found. The Visual Basic code for this calculation is shown in Appendix A. Figure 6.2 shows the results of this calculation as a function of the data pressure. Excel's "LINEST" function was used to generate the best-fit equation to these results. This is shown here for clarity:

$$m_{loss} = -3.75 \times 10^{-13} P_f^2 + 2.58 \times 10^{-10} P_f + 1.22 \times 10^{-7} \quad (6-6)$$

As can be seen in Figure 6.2, beyond approximately 1000 kPa the mass loss became negative. It was at this point that the mass loss was assumed to be zero.

At lower pressures the mass loss diagram shows order of magnitude variations in the mass loss. This is a result of variations in the data and the calculations performed on this data. The ideal data set would conform to the ideal gas equations, but due to the data collection procedures and the nature of the system this did not happen. The process, being a point to point calculation, would over-estimate the mass loss for one point and at the next correct for this extra mass and under-estimate the losses. By applying a best-fit curve to the calculated mass loss, the errors would be averaged and the resulting curve would give a better approximation of the mass loss.

This equation, although derived with motoring data only, was used for all subsequent calculations. There may have been minimal errors introduced because of this, but their effect would be slight because the total mass loss was small compared to the total mass of fuel and air in the system.

A second part of the mass loss problem was how to calculate the fuel mass loss. The solution was fairly simple and relied on several assumptions that held true throughout this study. The first was that the only loss came from vapor; therefore no liquid fuel left the system. Secondly, when the fuel evaporated it instantaneously mixed with the air in the system, making a homogeneous mixture. Using these assumptions, the mass loss could be calculated. In the case of motoring the calculation is simply

$$m_{air} = m_i - m_{loss} \quad (6-7)$$

When injection occurred, the calculation became more complicated because  $m_{loss}$  was the total mass loss from the system. The loss needed to be divided into two constituents, namely fuel and air. Since the mixture was assumed to be homogeneous, the mass loss of each substance would be proportional to its percentage of the total mass. So,

$$m = m_x - m_{loss} \left( \frac{m_x}{m_{tot}} \right) \quad (6-8)$$

where the subscript  $x$  denotes the substance and  $m_{tot}$  is the total mass of the vapor in the system.

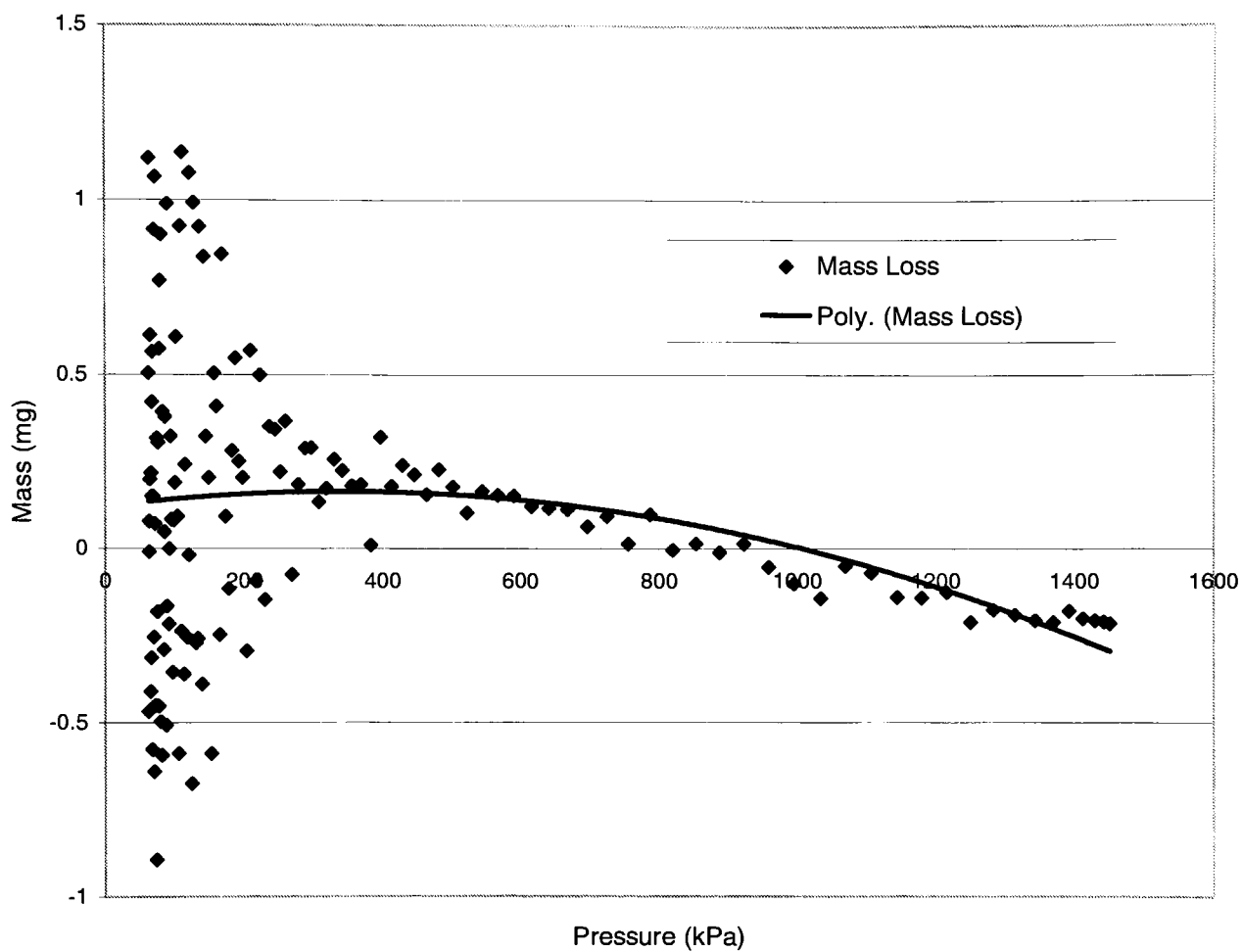


**Figure 6. 2 Mass Loss as a Function of In-Cylinder Pressure**

### 6.2.3 Heat Transfer

Another factor that would influence the behavior of the system is the heat transferred between the piston-cylinder assembly and the mixture of liquid fuel and vapor. This heat transfer would cause a change in temperature of the mixture, which is an important parameter in the FIGE process. This heat transfer problem was complex for two reasons. Calculation of the heat transfer coefficient for the cylinder-vapor interface was the first complexity. The second was that the system was dynamic and the surface area was always changing.

The Engineers at Delphi made the calculation of the heat transfer coefficient much less complex. They evaluated this parameter for a similar engine in a previous study and provided the results. Figure 6.3 shows the results, or the heat transfer coefficient with respect to the crank angle of the engine. Excel was used to calculate equation 6-9, a best-fit approximation of the data; this will be used in the remainder of the study.

$$\begin{aligned} h_T &= 0.09, CA < 240^\circ \\ h_T &= 2.32 \times 10^{-7} CA^3 - 0.00017 CA^2 + 0.041752 CA - 3.39289, \quad (6-9) \\ &CA \geq 240^\circ \end{aligned}$$

where  $CA$  is defined as the crank angle in degrees.

Before looking into the dynamic nature of the system, it was necessary to know the parameters needed to solve the heat transfer problem. Equations 2-7 and 2-16 show everything needed to evaluate the change in temperature of the fuel vapor mixture.

$$Q = h_T A_s (T_s - T_\infty) \quad (2-7)$$

$$Q = mc_p \Delta T \quad (2-16)$$

The following equation is the result of combining these equations and solving for  $\Delta T$  :

$$\Delta T = \frac{h_T A_s (T_s - T_\infty)}{mc_p} \quad (6-10)$$

The two unknown factors were the surface area,  $A_s$ , and the surface temperatures,  $T_s$ . The calculation of these variables was difficult because of the dynamics of the system.

The surface area consisted of three regions, two of which were static while the third was dynamic. The area of the piston head was measured to be approximately 43 cm<sup>2</sup>. The second constant area region was that of the area above the top of the stroke in the clearance volume region. The surface area in this region was approximately 55 cm<sup>2</sup>. These values were measured and provided by the test engineers at Delphi.

The final surface area was that of the walls of the cylinder. As the volume of the cylinder changed, this surface area also changed. In order to calculate this surface area some basic geometric equations of a cylinder were needed. These were:

$$V = \pi r^2 h \quad (6-11)$$

$$A_s = 2\pi r h \quad (6-12)$$

where  $V$  is the cylinder volume,  $r$  is the cylinder radius,  $h$  is the height of the cylinder and  $A_s$  is the lateral surface area of the cylinder. Also note that the volume in the engine cylinder, that is, the volume associated with the cylinder wall surface area, is

$$V_{cyl} = V_i - V_{clear} \quad (6-13)$$

where  $V_i$  is the known total volume of the system and  $V_{clear}$  is the clearance volume.

By relating equations 6-11 and 6-12 to the engine and letting  $B$  equal the bore of the engine, it was clear that

$$r = \frac{B}{2} \quad (6-14)$$

These equations were combined to get

$$V_i - V_{clear} = A_s \frac{B}{4} \quad (6-15)$$

Solving for  $A_s$ :

$$A_s = 4 \frac{(V_i - V_{clear})}{B} \quad (6-16)$$

So, with any given volume, the surface area could be calculated.

Each surface area then had to be associated with a temperature. For the static areas the temperature was easy to find; the engine could be probed with thermocouples in these areas. Delphi provided these readings. The piston head area temperature was 483 K and the cylinder head area temperature was 533 K.

Two assumptions had to be made to calculate the wall temperature. The first was that the above two temperatures were the minimum and maximum in cylinder surface temperatures, respectively. The second assumption was that the temperature varied linearly from the minimum to the maximum along the wall. From these assumptions, the surface temperature equation was derived.

Using the basic equation of a line,

$$y = mx + b \quad (6-17)$$

surface temperature with respect to volume could be calculated as follows:

$$T_s = m_s V_i + b \quad (6-18)$$

provided that the slope of the line,  $m_s$ , and the temperature intercept,  $b$ , were known. The slope varied linearly from the minimum temperature at the total volume to the maximum temperature at the clearance volume. So,



$$m_s = \frac{T_{\max} - T_{\min}}{V_{clear} - V_{tot}} \quad (6-19)$$

Using this calculated slope the intercept could be calculated:

$$b = T_{\max} - (m_s V_{clear}) \quad (6-20)$$

Therefore, the minimum cylinder wall temperature could be calculated as a function of volume.

Since the temperature varied linearly along the wall, the average wall temperature was

$$T_s = \frac{(m_s V_i + b) + T_{\max}}{2} \quad (6-21)$$

Combining these equations with equation 6-10, the value of  $\Delta T$  could be found at each volume increment. Then the initial temperature was calculated as follows:

$$T_i = T_i - \Delta T \quad (6-22)$$

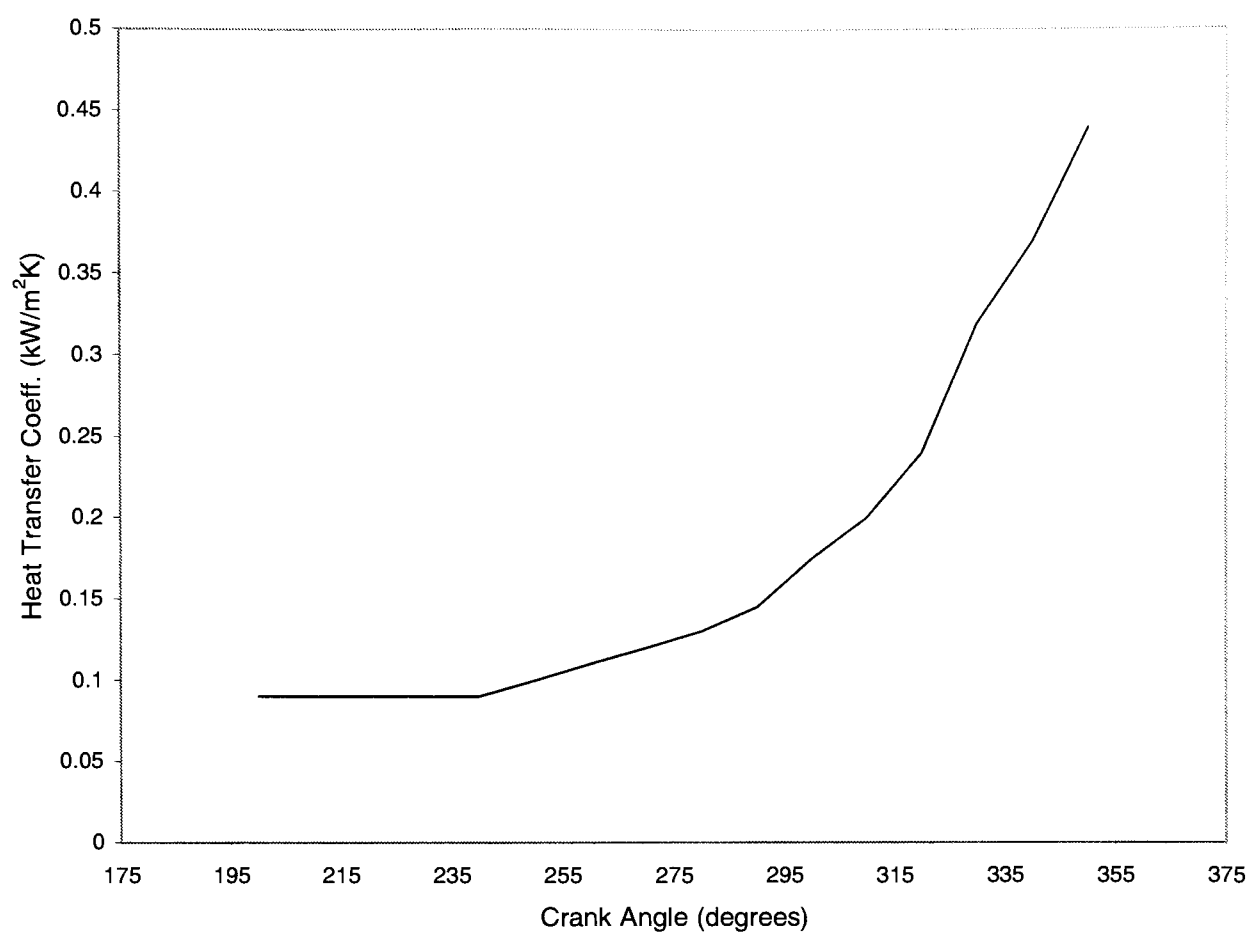


**Figure 6. 3 Heat Transfer Coefficient as a Function of Crank Angle**

#### 6.2.4 Residuals

Once again, the system used in this study was not an ideal system. If it were, complete combustion of the fuel would occur. Due to the nature of the system, only partial combustion occurred and exhaust and residual gases were expelled from the engine. Unfortunately, all of these residuals were not purged from the engine during the exhaust stroke. The result was a mixture of air and residual gases in the cylinder. This had to be compensated for in the FIGE model calculations.

The first step in calculating the residual gases was to measure the amount of residuals in the exhaust. This was accomplished by using the Pierburg process during the procedure to collect the emissions from the engine. The result of this process was the mass of each residual for the entire test cycle. In order to reach the final goal of calculating the specific heat ratio for the residuals, the percentage of the total residual mass was calculated for each residual gas. These included  $N_2$ ,  $NO$ ,  $CO$ ,  $CO_2$ , and  $O_2$ .

The specific heat ratio of a substance at a given temperature was calculated using the specific heat values of the substance at that temperature. So, a percentage of total mass was known for each residual gas; this percentage was assumed to remain constant throughout the study. Therefore, by knowing the total mass of residuals within the cylinder, the specific heat ratio for the residuals could be calculated.

It was assumed that 10% of the total mass of air within the cylinder consisted of residuals. Since the initial mass of air in the cylinder was known, the residual mass was calculated:

$$m_{resid} = 0.1m_i \quad (6-23)$$

For each residual gas a  $c_p$  and  $c_v$  value could be calculated for a range of temperatures. By multiplying each of these values by the associated mass percent and adding the subsequent values together, then dividing by the total mass, a  $c_p$  and  $c_v$  of the residual was found:

$$c_{p,resid} = \frac{\sum_a m_a c_{p,a}}{m_{resid}} \quad (6-24a)$$

$$c_{v,resid} = \frac{\sum_a m_a c_{v,a}}{m_{resid}} \quad (6-24b)$$

where the index "a" is for each corresponding residual gas. This calculation is shown in Appendix B. This defined the specific heat functions for the residual gases. These functions can be used throughout the FIGE process.

### 6.2.5 Putting it All Together

The FIGE process has been briefly presented up to this point and several parameters that affected the overall performance of the model have also been explained. These two aspects had to be combined so the model matched the actual data.

The first step in the process was to calculate the initial mass in the system. This was done using equation 2-3 and the initial values of temperature, volume, and pressure. Then the residual mass was calculated using equation 6-23. Using the mass loss function, the mass loss of the system was calculated. Then the mass loss of each constituent was calculated.

Heat transfer equations were then used to reduce the initial temperature of the system. At this point, the new initial pressure of the system was calculated from the partial pressure of each of the constituents. With this new pressure and temperature, the FIGE process was used to calculate the final temperature and pressure for each crank angle. This process is shown in Figure 6.4.

One key ingredient was missing, however. The fuel had yet to be introduced into the system. The remaining sections will detail how this was accomplished and show the completed model.

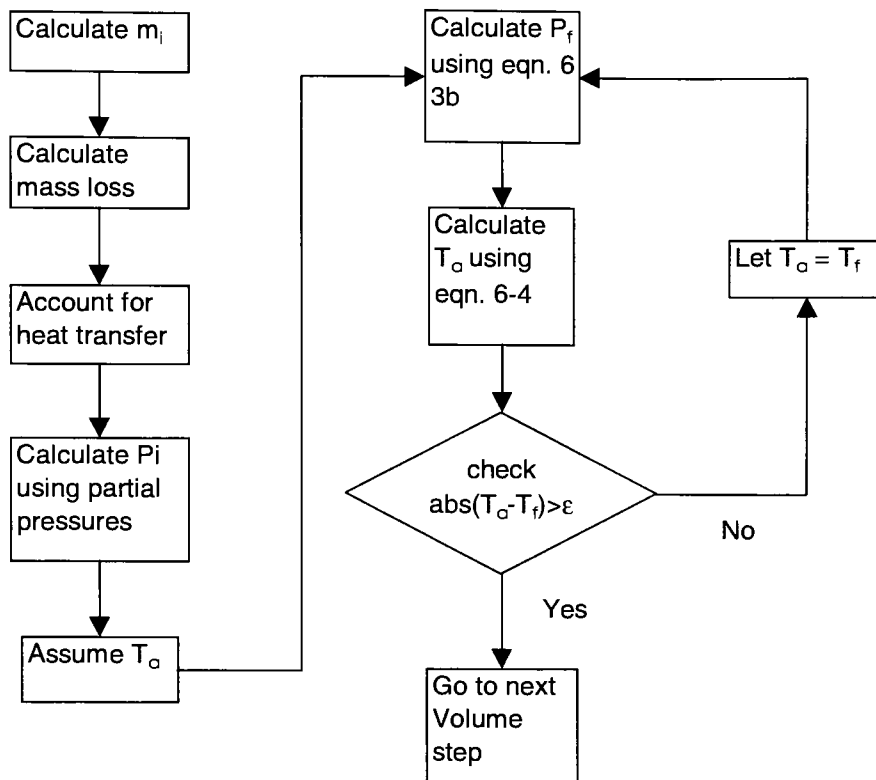


**Figure 6. 4 FIGE Process Flow Including Losses**

### *6.3 Fuel Injection*

Once again, the goal of this study was to determine the amount of fuel evaporated in the cylinder of a direct injection gasoline engine prior to ignition. Developing a simple, inexpensive technique is necessary because all the current techniques for doing this are expensive and difficult to use. In a direct injection engine liquid fuel is injected directly into the cylinder during the compression stroke. This fuel must evaporate prior to combustion. Otherwise, combustion will not occur properly and engine performance will be less than optimum.

So far the FIGE model had not taken into account the fuel being injected into the cylinder. This was the most important parameter to the study and affected the calculations in the model. These effects will be discussed in greater detail in this section. Several assumptions needed to be made prior to explaining the evaporated mass calculations. These assumptions were: fuel was injected completely and instantaneously into the cylinder during several crank angle degrees, the volume of fuel injected into the cylinder was negligible, and when the fuel evaporated it mixed homogeneously with the air in the cylinder. By combining these assumptions and the FIGE process, a technique was developed to calculate the evaporated mass.

#### **6.3.1 Fuel Injection and the FIGE Process**

As discussed in Section 6.2, there were many parameters affecting the outcome of the FIGE process. It was shown that these parameters could be added to the model provided that the values associated with the new parameters were known and the

constituents were in vapor form. When the fuel was injected it was a liquid. After the fuel evaporated, its mass was unknown. Therefore, this mass needed to be calculated in order to complete the model.

Once the evaporated mass was known, the FIGE process had the following flow: the mass of the vapor in the cylinder was calculated by adding the residual mass, the mass of the evaporated fuel, and the mass of air; mass loss calculations were performed and mass was subtracted from each of these masses; heat transfer was accounted for by using the heat transfer equations and by reducing the initial temperature; the partial pressure of each of the constituents was calculated and summed for the total pressure; the FIGE process was then used to find the pressure at the next crank angle degree.

This process was performed for every change in volume. Prior to injection, the mass of the evaporated fuel was zero. For the first step after injection occurred, the evaporated fuel mass was unknown, but there was a calculated pressure and a corresponding data pressure point. These differed because of the unknown mass of fuel. The remainder of this section will discuss the details of how the evaporated mass was calculated.

### 6.3.2 Deriving the Evaporated Mass Equation

The data pressure at every point consisted of the sum of the partial pressures of the air, residual vapors, and evaporated fuel. The FIGE process, to this point, had taken into account the partial pressure of the air and the residuals. Any difference in pressure between the data pressure and that calculated by the FIGE process was a result of the evaporated fuel. The partial pressure of the evaporated fuel could be calculated using



equation 2-3, provided that the mass of the fuel was known as well as the temperature. The partial pressure of the evaporated fuel could also be calculated by subtracting the pressure calculated by the FIGE process from the data pressure.

$$P_{fuel,1} = \frac{m_{fuel} R(fuel) T}{V_f} \quad (6-25a)$$

$$P_{fuel,2} = P_{calc} - P_{data} \quad (6-25b)$$

The mass of the evaporated fuel had to be calculated. Noting the flow of the FIGE process, it is evident that any losses due to leaks in the system had been accounted for. Therefore, the in-cylinder mass remained constant for the next step. Since the mass of the injected fuel was known, two associated pressure values could be calculated. These were the partial pressure of the fuel vapor with the entire mass of fuel in vapor form and the same partial pressure with no evaporated fuel. This value was only zero at the initial injection crank angle; after some fuel had evaporated there was an associated partial pressure. The actual mass of the fuel had to be between these two extremes.

The mass could be calculated in one of two ways: the brute force method or the bisection method. The brute force method simply tests every possible value of mass between the two extremes and tries to determine which will give the correct pressure. This method is slow and requires a lot of processing power. The bisection method is slightly more difficult but gives accurate results in a shorter period of time; it was the method used in this study.

The bisection method will be described briefly in general terms, and then the proper equations will be implemented to calculate the mass. The bisection method uses the extreme values of a function to find that function's roots. The goal is to find a value,

$x$ , between  $x_a$  and  $x_b$  that makes the function  $f(x)=0$ . This can be accomplished providing that the function only changes sign once in this interval.

Once  $x_a$  and  $x_b$  have been selected,  $f_a=f(x_a)$  is calculated. The value of the function at the midpoint of the interval is calculated as follows:

$$x_m = \frac{x_a + x_b}{2} \quad (6-26a)$$

$$f_m = f(x_m) \quad (6-26b)$$

The product of the two functions is calculated:

$$B_p = f_a \times f_m \quad (6-27)$$

If the result of this calculation is positive, the root of the equation is between  $x_m$  and  $x_b$ ; otherwise the root is between  $x_a$  and  $x_m$ . So when  $B_p > 0$ ,  $x_a$  is set equal to  $x_m$ , and when  $B_p < 0$ ,  $x_b$  is set equal to  $x_m$ . The difference between  $x_a$  and  $x_b$  is calculated. If it is sufficiently small, the root can be calculated by linear interpolation between  $x_a$  and  $x_b$  or by simply using  $x_m$  as the root. The process is continued until the difference between  $x_a$  and  $x_b$  is sufficiently small.

Applying this to the evaporation process, the mass of the evaporated fuel could be calculated. The necessary components were mass, which had a maximum and minimum value, and a function that could be used to find the necessary results. This function had to be developed from the known pressure difference between the actual pressure and the calculated pressure.

The form of the function that needed to be developed was  $f(x)=0$ . An accurate model needed to be developed; therefore, the difference between the two partial pressures of the evaporated fuel had to be minimized. So,

$$P(m_{fuel}) = P_{fuel,2} - P_{fuel,1} = 0 \quad (6-28)$$

In equations 6-25a, 6-25b, and 6-28 all the variables were known except for  $m_{fuel}$  and  $T$ . The variable  $m_{fuel}$  was going to be solved for, but  $T$  was unknown. The temperature,  $T$ , was the final temperature of the vapor inside the cylinder. This had to be found using equations of heat transfer. The resulting equation for  $T$  was a function of the unknown evaporated fuel mass.

There are several reasons heat transfer could be used to determine the final temperature of the vapor. The first reason is that during the process of calculating the evaporated fuel mass, the volume of the cylinder was constant. The FIGE process was used to calculate the change in pressure from point 1 to point 2; the evaporation was assumed to be occurring at point 2 only. It is assumed that because the fuel is evaporating, the in-cylinder temperature remains constant. As a result of this constant temperature, the heat required to evaporate the liquid was directly related to the convective heat transfer from the cylinder surface to the air/fuel mixture.

There were two components of heat transfer acting on the vapor that had to be accounted for in this study. These were convective heat transfer from the cylinder walls to the vapor, and the amount of heat required to change the liquid fuel into vapor, known as the latent heat of vaporization. These two components were combined to balance the heat transfer in the system.

Convective heat transfer was used to find the heat transfer between the cylinder walls and the fuel. Equation 2-7 was used for this process; it is rewritten as:

$$Q_c = hA(T_s - T_f) \quad (6-29)$$

Once again the geometric properties of the cylinder were used to perform the actual calculation.

The second form of heat transfer, the latent heat of vaporization, was needed to calculate the amount of heat required to change the fuel from liquid to gas. This heat was simply the mass of the fuel that had evaporated multiplied by the latent heat of vaporization:

$$Q_l = m_{fuel} L_v \quad (6-30)$$

Now that the types of heat transfer had been established, they had to be combined into a form useful to the Bisection Method. As stated earlier and as an assumption of this model, the heat required to evaporate the fuel is equal to the amount of heat transferred to the air/fuel mixture by convection. This is the governing heat transfer equation:

$$Q_c = Q_l \quad (6-31)$$

Therefore,

$$hA(T_s - T_f) = m_{fuel} L_v \quad (6-32)$$

Solving for  $T_f$ ,

$$T_f = T_s - \frac{m_{fuel} L_v}{hA} \quad (6-33)$$

By combining equations 6-33 and 6-25a, then substituting into equation 6-28, it is possible to use the Bisection Method to solve for the evaporated fuel mass.

## 7. RESULTS

Three portions of the development of the FIGE process have been addressed. These are the initial FIGE process development, the adjusting and calibration of the model, and the implementation of a process to measure the mass of evaporated fuel. The results of these sections will be presented here.

### *7.1 FIGE Development*

The development process used motoring data after injection had occurred. Using the FIGE process as described in Section 6.2, the pressure at each corresponding crank angle was calculated. Figure 7.1 shows these FIGE pressure data with respect to the cylinder volume. Also included in Figure 7.1 are the corresponding motoring data provided by Delphi.

Figure 7.2 shows the percent error of pressure values for each corresponding data point. The standard deviation of these values was 3.97 as calculated using Excel's "STDEV" function.

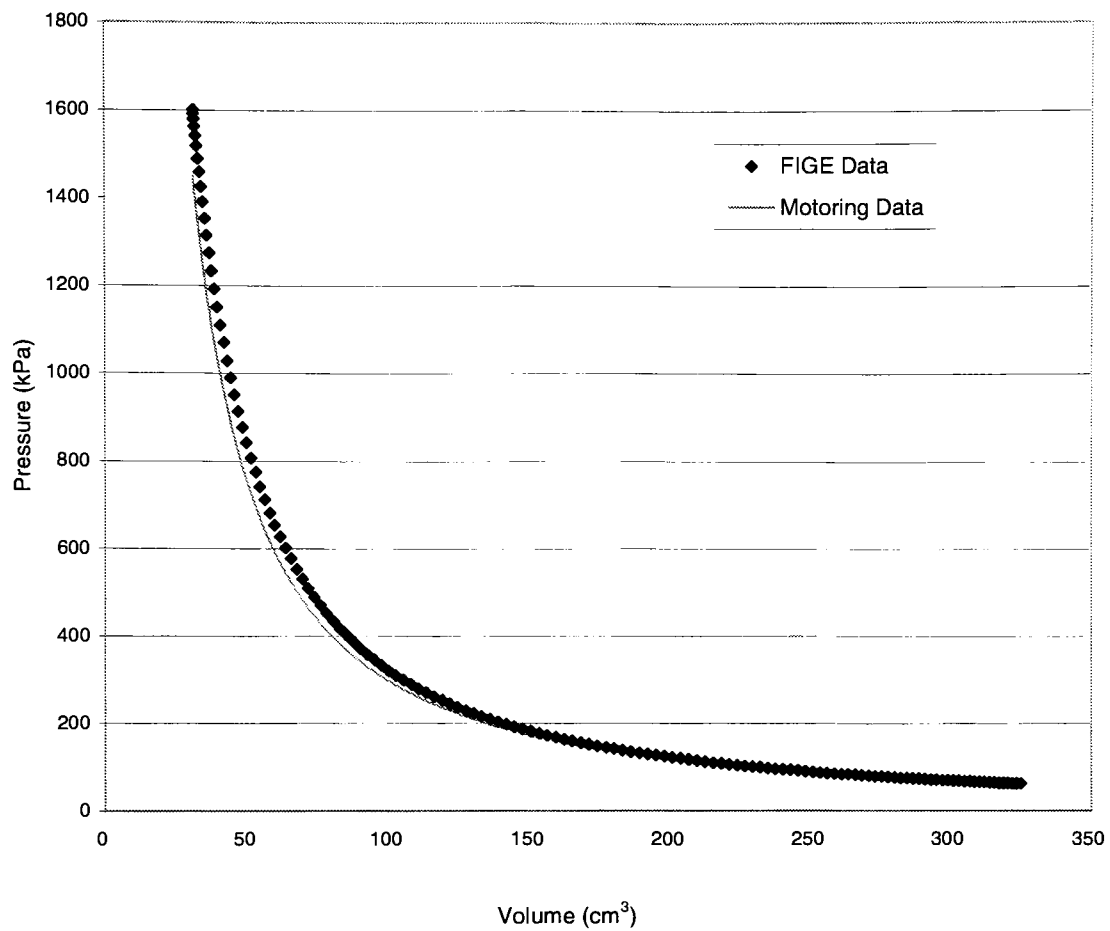


**Figure 7. 1 A pV Diagram of FIGE Motoring Data Without Losses**

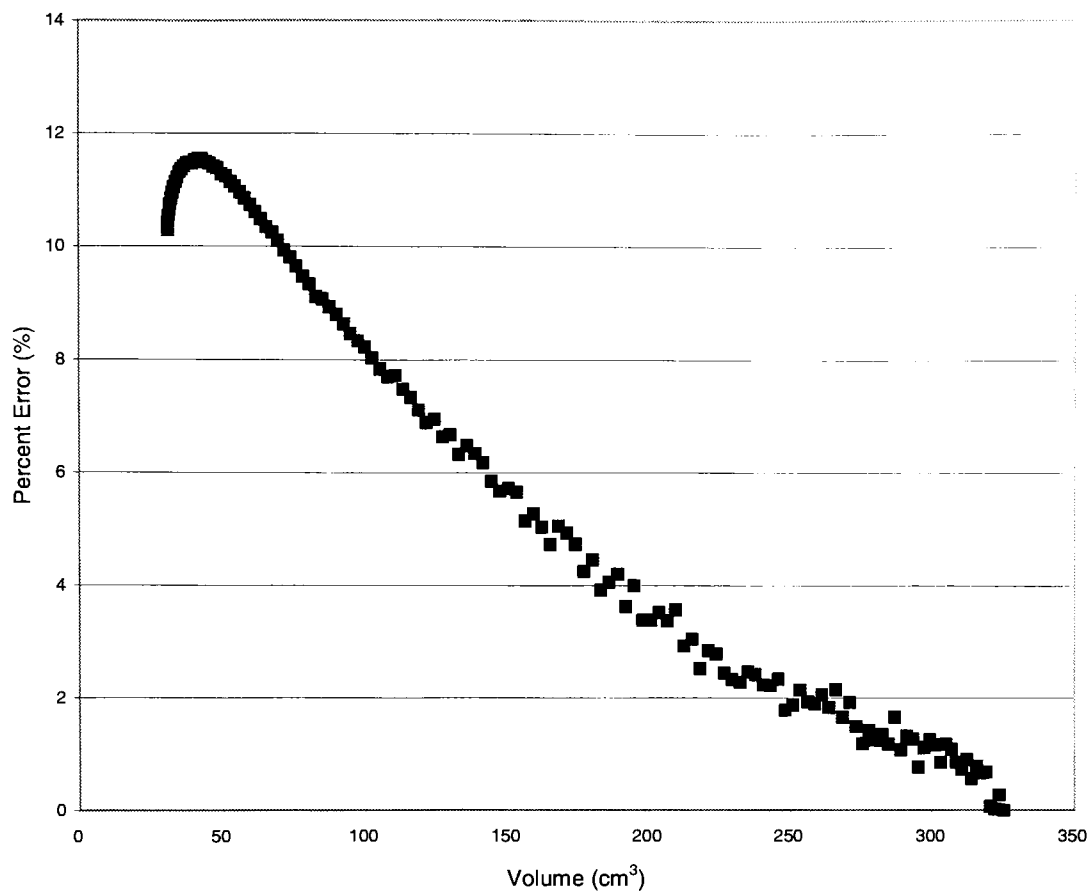


**Figure 7. 2 Percent Error in Pressure as a Function of Cylinder Volume**

## *7.2 FIGE Calibration*

The second step in development was to calibrate the model. This was done by adding residuals, heat transfer, and mass loss to the FIGE process. Again, motoring data after injection had occurred was used. Figure 7.3 shows the FIGE pressure data, along with the motoring data, with respect to cylinder volume.

A standard deviation of percent error in pressure of 0.65 was calculated using the percent error data shown in Figure 7.4.



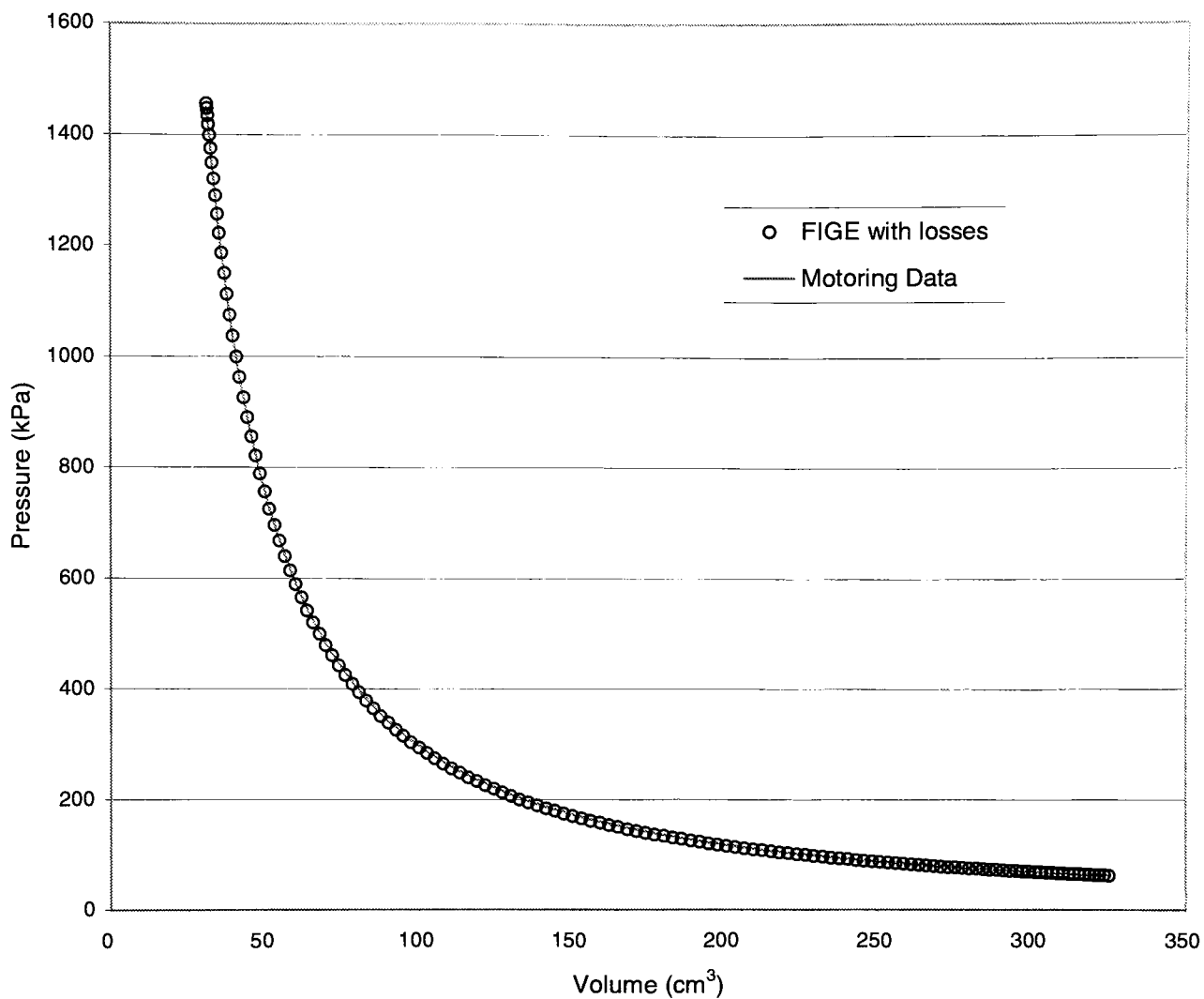


**Figure 7. 3 A pV Diagram of FIGE Motoring Data Including Losses**

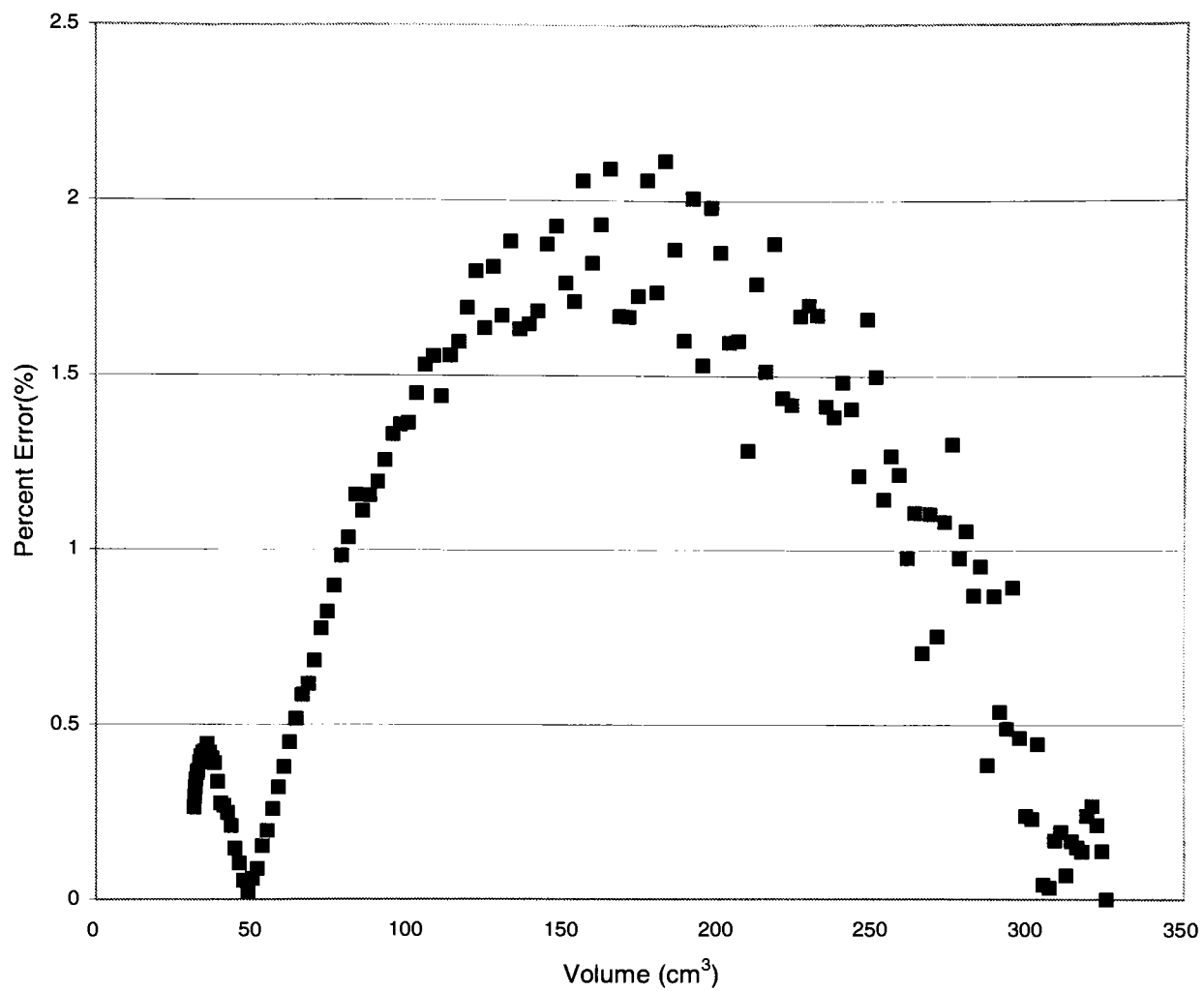


**Figure 7. 4 Percent Error in Pressure as a Function of Cylinder Volume Including Losses**

### *7.3 Evaporated Fuel Mass Calculation*

Once the model was calibrated for losses and residuals, a procedure was defined to evaluate the amount of evaporated fuel in the cylinder prior to combustion. Again, the results of this calculation will be shown in a pV Diagram (Figure 7.5) and a Percent Error in Pressure Chart (Figure 7.6). The standard deviation of the percent error in pressure of 4.74 was calculated from the data in Figure 7.6.

Figure 7.7 shows the evaporation profile of the fuel in the cylinder.

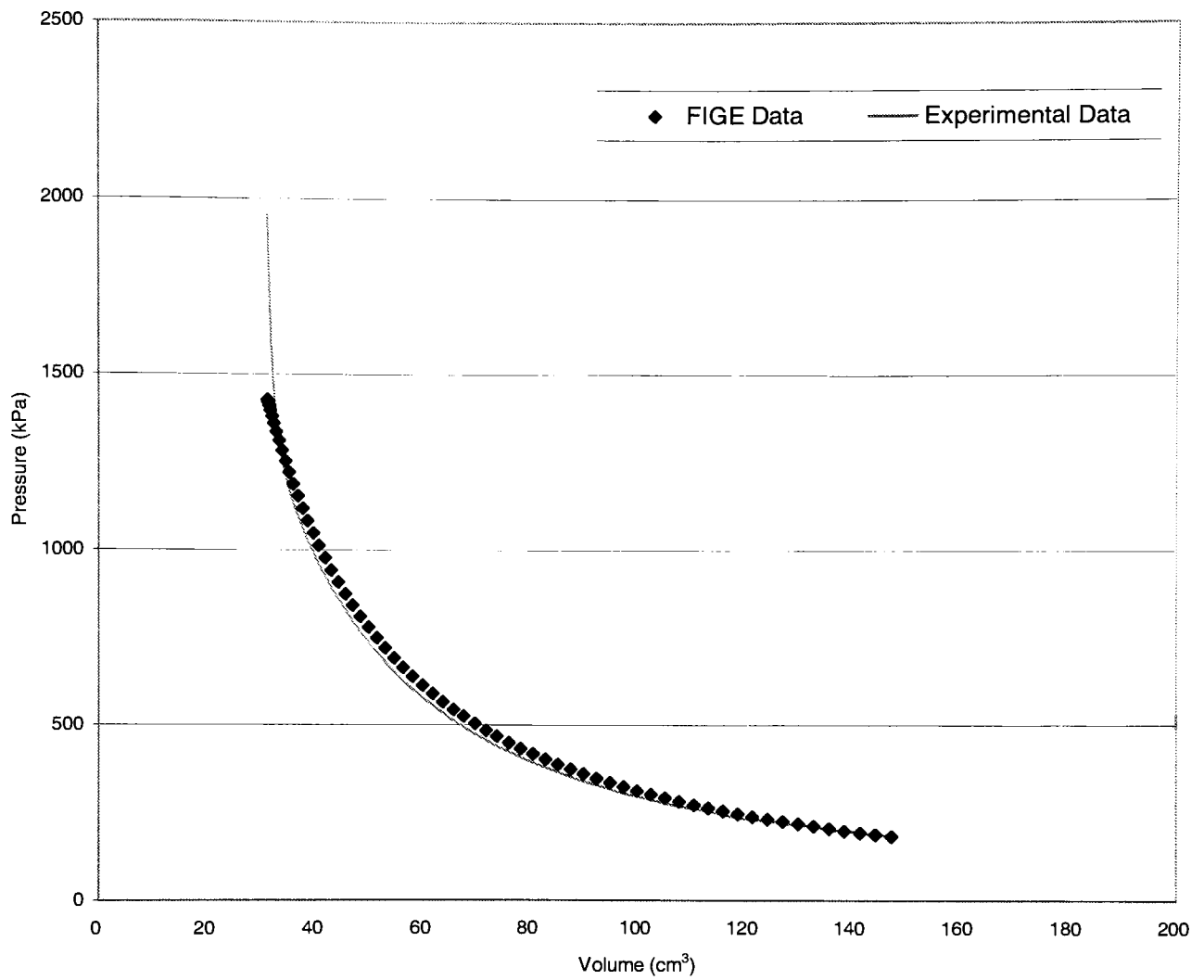


**Figure 7. 5 A pV Diagram of Fuel Injected FIGE Data**

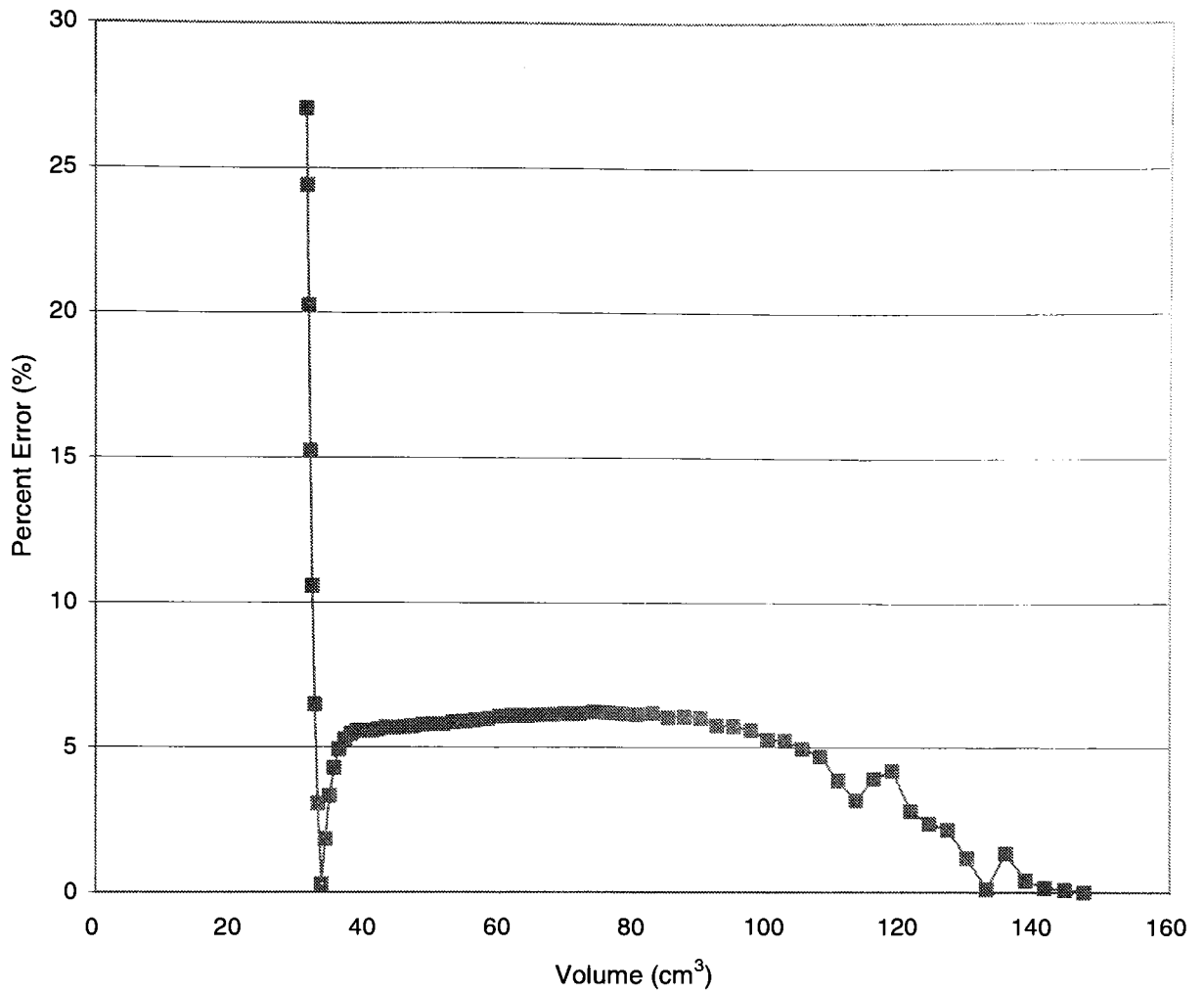


**Figure 7. 6 Percent Error in Pressure as a Function of Cylinder Volume for Fuel Injection**

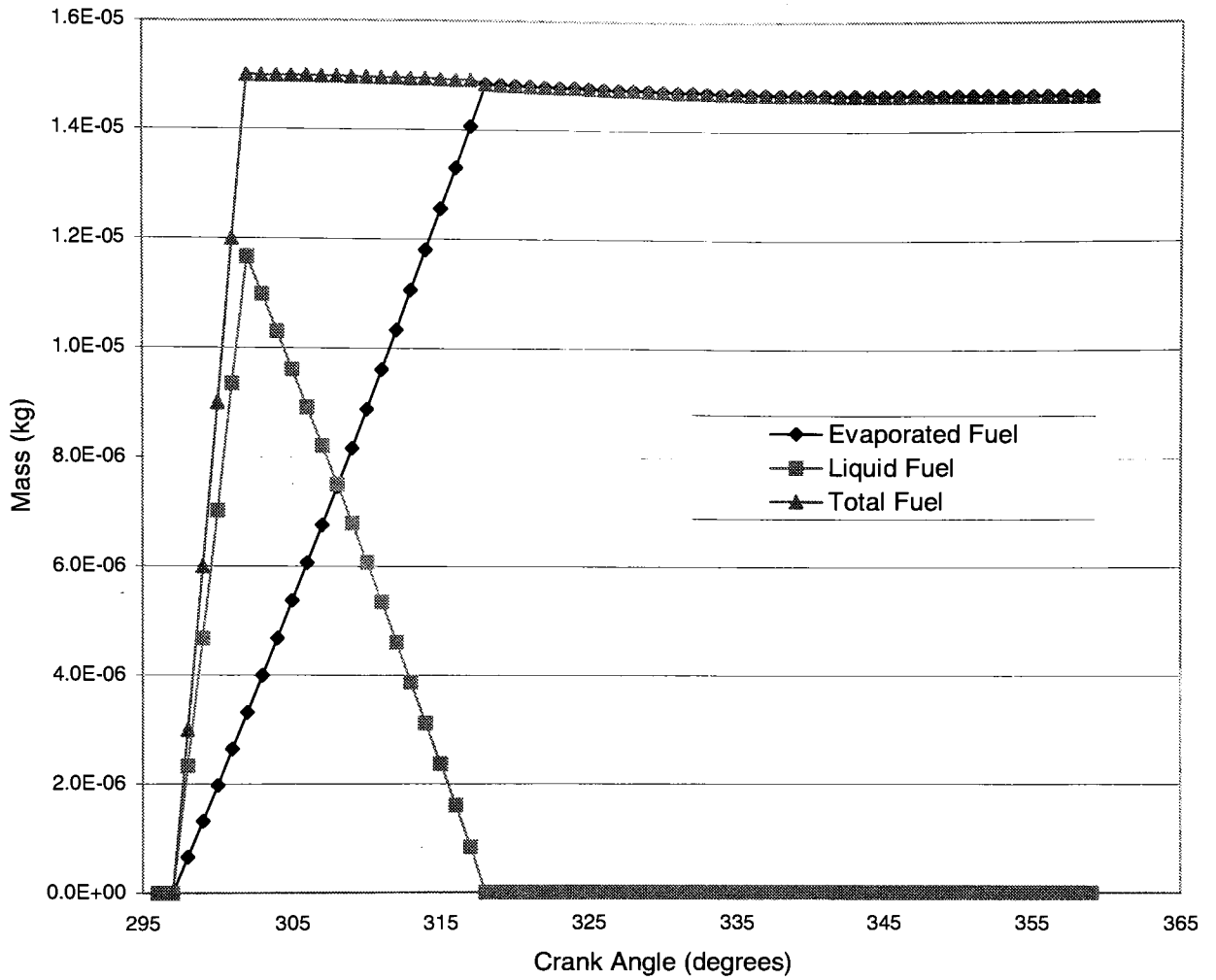


**Figure 7. 7 Injected Fuel Evaporation Profile**

## 8. CONCLUSIONS AND RECOMMENDATIONS

The goal of this study was to develop a simple, inexpensive technique to calculate the amount of evaporated fuel present in the combustion chamber of an engine at the time of ignition. The model that was developed was based on the specific heat ratio of fuel vapor and pressure changes in the combustion chamber. A single cylinder direct-injection spark-ignition internal combustion engine was used to provide the data used to build and evaluate the model. The results provided in Section 7 show that the technique accurately predicts pressure values for the motoring case without injection. The results from the injection case are not as accurate as the motoring cases; there are many items which factor in to this reduced accuracy. These will be explained in detail in the remainder of this section.

There are three important factors that determine the success of this study. These are developing a technique that is simple and inexpensive and provides adequate results. The simplicity and cost effectiveness of the technique are due to the fact that it used a small engine and only pressure and residual data from that engine were collected. The engine used to collect data was a typical test engine used for pressure tests; there were no special adjustments or calibration required in order for the engine to perform properly. Also, the pressure and residual data were acquired using standard test and data retrieval equipment. The requirements of a simple, inexpensive technique were achieved because only existing equipment and techniques were used for data collection and there was no development time or effort needed to acquire the data needed to perform the calculations.

The remainder of this section will provide explanations of the results as well as how these results correlate to the physical model. Recommendations for future studies

will be provided. The model has a solid basis, but several factors could be modified to improve the results for the case of injection.

### *8.1 The Motoring Case*

The FIGE process, the basis for the FIGE model, was shown to be a valid process. Figure 7.1 shows results which are based solely on this process. The standard deviation of 3.97 shows that these results closely resemble the actual data.

By taking a closer look at Figure 7.1, it is evident that the FIGE process alone does not give adequate results. The model starts by using the actual pressure at the effective closing angle as the initial pressure. In the figure this is the point farthest to the right, corresponding to the largest volume. By following the curve to the left, it can be seen that the difference between the data pressure and the calculated pressure begins to increase. This shows that the FIGE model is predicting pressures which are greater than the data pressures. The divergence of the data can be seen more clearly in Figure 7.2, the percent error data. Again, starting with the point farthest to the right and moving left, the percent error in pressure increases indicating there is a discrepancy between calculated and experimental data. This leads to the second part of the model, the calibration and addition of losses.

Once the model was calibrated and the losses from the system were calculated, the results of the model improved significantly. A comparison of the standard deviations shows this improvement, 3.97 without losses and 0.65 with the losses. Figures 7.3 and 7.4 show that the calculated pressure matches the data pressure nearly exactly throughout the cycle. The largest percent error is slightly larger than 2%, which corresponds to



approximately 4 kPa, a measurement within the accuracy of the measuring instrumentation.

The FIGE process is a very accurate tool for calculating the pressure values during a motoring cycle. The model can closely predict the pressure values and is a good building block for the injection portion of the model. There are several key areas that could be improved to enhance the results. These include the calculation of the initial temperature, the mass loss, and the residuals.

The initial temperature calculation could be improved by implementing a highly sensitive thermocouple in the cylinder. This thermocouple would record in-cylinder temperatures during the compression stroke and would provide a better temperature profile for the model. Rather than calculating the temperature at each step, the temperature profile would be used. This was not done due to the prohibitive cost of purchasing and implementing such a device.

Rather than using empirical results to calculate the mass loss, specific mass loss equations could be derived. These equations would take into account the density of the fuel, the leakage area, and engine characteristics during the cycle. As stated earlier, this would be a very complex task, but would result in an extremely accurate mass loss profile.

The residual calculation is a difficult calculation and could be improved. Because of the complexity of the calculation and the numerous residuals accumulated in the cylinder, the calculation was simplified. All the residuals were lumped into a representative residual and this “summed” residual was used throughout the entire study. Taking into account each residual gas could improve the performance of the model.

## *8.2 The Fuel Injection Case*

The injection process as discussed in Section 6 relied on differences between data collected at Delphi and calculations made using the FIGE process. The FIGE process was used to calculate a pressure, which was then compared to the data collected by Delphi. Using this comparison, an evaporated fuel mass could be extrapolated. As noted in the previous section, there were slight errors involved in the FIGE calculation. Any small errors in this calculation would later be magnified by the evaporated fuel mass calculation.

The calibration process was aimed at reducing any errors that could occur. As shown by the results in Figures 7.3 and 7.4, the errors were minimized but still present. Figure 7.5 illustrates that the errors do propagate throughout the cycle. Again, by starting with the largest volume and following the curve, it is clear that the FIGE data begins to move away from the experimental data. The reason for this error propagation is that the final step in the FIGE model is to calculate a pressure based on the partial pressure of the air and fuel vapor calculated in the evaporation process. This final pressure is then used for the initial pressure for the next step. Any error in the initial step will still be seen in the following steps.

By comparing the data in Figures 7.3 and 7.5 it can be seen that the process does not begin at the same volume. Prior to using the evaporation process, the data was tracked beginning with the effective closing angle. After fuel was injected into the cylinder, another approach was taken to reduce errors. The calculations were started a few crank angle degrees before the injection crank angle, introducing minimal error into the system prior to beginning the calculations.

Another thing to note is that there are large errors in the pressure values calculated by the FIGE process as the piston is nearing TDC. These errors are due to two factors, the propagation of the previous errors and the large pressure differences between crank angles. When there are both fuel and air in the cylinder and the piston is nearing TDC, large pressure differences are created between successive crank angles. At these extreme conditions the model cannot accurately predict the pressure of the vapors because the mixture is moving away from ideal gas conditions.

This state does not occur until approximately 10 degrees before TDC. At this point in a typical engine, ignition would have already occurred or would occur within a few degrees. By discarding the few points near the end of the compression stroke, the overall fit of the FIGE data to the experimental data would improve. This can be confirmed by examining Figure 7.6. The average percent error would be slightly higher than 5% if the points corresponding to the lowest volume were eliminated.

Overall, the accuracy of the model is sufficient for this study, although, as mentioned above, there are several improvements that could be made to the model. One significant improvement would be to utilize more data points during the cycle. The current process only uses pressure measurements taken at every crank angle. By taking measurements at every half or quarter angle, the results could be improved significantly.

### *8.3 Evaporated Fuel Mass*

The goal of this study was to determine the amount of fuel present in the combustion chamber at the time of ignition. This was accomplished by creating an evaporation profile of the fuel in the cylinder. Figure 7.7 shows this evaporation profile.

The data used in this study was collected from a normally operating engine into which fuel was being injected. The fuel was not ignited at the end of the process; therefore the results are better suited for determining when ignition should occur rather than calculating the evaporated fuel mass at ignition.

There are three curves shown in Figure 7.7; each of these curves represents the injected fuel mass in various phases. The first phase is the total mass of the fuel in the cylinder. By reading the graph from left to right, it is evident that prior to injection (296 CA°) there is no fuel in the cylinder. As the compression stroke continues there is a steep rise in the slope of the line; this denotes fuel being injected. The fuel injection occurs from 298 CA° to 302 CA°. A relatively large mass of fuel is injected over a few crank angles.

Once again, it is important to note that there are losses in the system. The mass losses throughout the cycle can clearly be seen in the remaining portion of Figure 7.7. If there were no losses, the line would have remained horizontal at the total fuel until the piston reached TDC. As can be seen, this is not the case; the curve is a negative sloping line. The gentle pitch of this line indicates that the mass loss in the system is very slight and that at higher crank angles or higher pressures, the mass loss approaches zero.

The remaining two curves in Figure 7.7 are best described as complements to each other. One curve is the liquid fuel mass in the cylinder, while the other is the evaporation profile of the fuel mass. The ignition timing can be calculated by the second of these curves. Adding these two curves together results in the total fuel mass.

The liquid fuel curve is derived by subtracting the evaporated fuel profile from the total fuel mass curve; therefore the liquid fuel curve will not be discussed. The

evaporated fuel profile is the one that is most relevant to this study. There are three items that define the evaporation profile; these are the crank angle at which the evaporation begins, the nature of the evaporation curve, and the crank angle at which the evaporation is complete.

As noted earlier, fuel injection begins at 298 CA°; according to the FIGE process, the evaporation process should begin immediately. This is true as seen in Figure 7.7; at 298 CA° there is slightly less than 1 mg of evaporated fuel in the cylinder. The evaporation process continues for 20 CA°, where it ceases because the entire fuel mass has evaporated.

The chart shows that the evaporation process is linear; for each change in crank angle an equal amount of fuel is evaporated. This indicates that the rate of evaporation is constant regardless of the amount of fuel in the cylinder and regardless of the increased temperatures caused by compressing the vapor mixture.

Theoretically evaporation occurs at a constant temperature; therefore evaporation will occur as long as the temperature within the cylinder is higher than the evaporation temperature. Also, according to the heat transfer theory, the rate of evaporation is not dependent upon the volume of the evaporating liquid. As long as there is enough fuel mass present, evaporation will occur at a constant rate. The linear evaporation profile is a reasonable outcome for this model.

As stated earlier, the goal of this study is to predict when ignition should occur. Figure 7.7 shows that all the fuel in the cylinder has completely evaporated at 318 CA°. The ignition timing can be predicted because complete combustion will occur when a stoichiometric mixture of air and fuel is present in the cylinder. Provided that the amount

of fuel injected into the cylinder is the correct quantity to make the in-cylinder contents stoichiometric, the spark plugs should be fired at or shortly after 318 CA° in this specific cycle for optimum engine performance.

As noted earlier in this section the FIGE model is not as accurate for the case of fuel injection as it is for the motoring case. The accuracy would have increased if the final few points in the model were disregarded. Because the evaporation is complete prior to these points, the accuracy of the model is sufficient to predict the ignition timing within a few crank angle degrees.

The FIGE model does not include any information about wall wetting, spray formation, or fuel droplet size. These are important parameters in the direct-injection engine process. These factors will influence the ignition timing to some degree. The ignition timing predicted by the model should only be used as a starting point for experimentation.

In conclusion, this model shows how pressure data and simple experimentation can be used to predict the ignition timing in a direct-injection fuel-injected spark-ignition engine. The FIGE model uses pressure data, ideal gas laws, and information about the specific heat ratio of the air/fuel vapor mixture to predict the ignition timing within a few crank angle degrees.

## REFERENCES

- Alger, Terrence, Matthew Hall, and Ronald Matthews, Fuel Spray Dynamics and Fuel Vapor Concentration Near the Spark Plug in a Direct-Injected 4-Valve SI Engine Proc. Direct Injection SI Engine Technology, Detroit, 1999. Warrendale, PA: Society of Automotive Engineers, Inc., 1999.
- Fan, L., G. Li, Z. Han, and R. D. Reitz, Modeling Fuel Preparation and Stratified Combustion in a Gasoline Direct Injection Engine Proc. Direct Injection SI Engine Technology, Detroit, 1999. Warrendale, PA: Society of Automotive Engineers, Inc., 1999.
- Incropera, Frank P., and David P. Dewitt, Fundamentals of Heat and Mass Transfer 4<sup>th</sup> ed. New York: John Wiley & Sons, Inc., 1996.
- Ipp, Wolfgang, Volker Wagner, Hanno Kramer, Michael Wensing, Alfred Leipertz, Stefan Arndt, and Amar K. Jain, Spray Formation of High Pressure Swirl Gasoline Injectors Investigated by Two-Dimensional Mie and LIEF Techniques Proc. Direct Injection SI Engine Technology, Detroit, 1999. Warrendale, PA: Society of Automotive Engineers, Inc., 1999.
- Keller, Frederick J., W. Edward Gettys, and Malcolm J. Skove, Physics 2<sup>nd</sup> ed. New York: McGraw-Hill, Inc., 1993.
- Moran, Michael J. and Howard N. Shapiro, Fundamentals of Engineering Thermodynamics 3<sup>rd</sup> ed. New York: John Wiley & Sons, Inc., 1995.
- Newton, K., T. Garrett, and W. Steeds, The Motor Vehicle 12<sup>th</sup> ed. Oxford: Butterworth-Heinemann Linacre House, Jordan Hill, 1996.
- Parrish, Scott E., and Patrick V. Farrell, The Influence of Injection Timing on In-Cylinder Spray Characteristics in a Direct-Injection Spark-Ignited Engine Proc. 1997 Fall Technical Conference, ASME. Madison, WI: Department of Mechanical Engineering University of Wisconsin-Madison, 1997.
- Robinson, C. William, Engine Research at Sandia's Combustion Research Facility Proc. 1996 Fall Technical Conference ASME. Livermore, CA: Automotive Programs Department Sandia National Laboratories, 1996.
- Stone, Richard, Introduction to Internal Combustion Engines 2<sup>nd</sup> ed. Warrendale, PA: Society of Automotive Engineers, Inc., 1992.
- Witze, Peter O., "Diagnostics for the Study of Cold Start Mixture Preparation in a Port Fuel-Injected Engine" Sandia National Laboratories, 1999.

## APPENDIX A. MASS LOSS CALCULATION

The following is the Visual Basic code for the mass loss calculation. Explanations of the code are italicized.

```
Sub MassLossCalc()  
Dim CaliSheet As Worksheet           initialize variables  
Dim Pstart, Vstart, Tstart As Range  
Dim Press_i, Vol_i, Vol_f, Temp_f, Press_f, GammaL as Double  
Dim Press_calc, mass_f, mass_calc, massloss as Double  
  
Set CaliSheet = Sheets("Calibration Data")   set object variables  
Set Pstart = CaliSheet.Range("o2")  
Set Vstart = CaliSheet.Range("n2")  
Set Tstart = CaliSheet.Range("p2")  
  
For s = 0 To 63  
    assign data from the "Calibration data" worksheet to the defined variable  
    Press_i = Pstart.Offset(s, 0)  
        Vol_i = Vstart.Offset(s, 0) * 0.000001  
        Vol_f = Vstart.Offset(s + 1, 0) * 0.000001  
        Temp_i = Tstart.Offset(s, 0)  
        Press_f = Pstart.Offset(s + 1, 0)  
  
    final temperature calculation  
    Temp_f = Press_f * Vol_f * Temp_i / (Press_i * Vol_i)  
  
    calculate gamma using the GammaAveMix function  
        GammaL = GammaAveMix(Temp_i, Temp_f, "Air")  
  
    final pressure calculation using equation 2-18  
    Press_calc = Press_i * (Vol_i / Vol_f) ^ GammaL  
  
    the next 2 lines are mass calculations based on equation 2-3  
        mass_f = Press_f * Vol_f / (Rvalue("Air") * Temp_f)  
        mass_calc = Press_calc * Vol_f / (Rvalue("Air") * Temp_f)  
  
    mass loss based on the difference in the calculated masses  
        massloss = mass_calc - mass_f  
  
    output to "Calibration data" worksheet  
    Tstart.Offset(s + 1, 0) = Temp_f  
        Tstart.Offset(s + 1, 1) = massloss  
Next s  
End Sub
```



## APPENDIX B. RESIDUAL MASS CALCULATIONS

$$c_p = R^* (a_1 + a_2 * T + a_3 * T^2 + a_4 * T^3 + a_5 * T^4)$$

	Temp Range	MW	a <sub>1</sub>	a <sub>2</sub>	a <sub>3</sub>	a <sub>4</sub>	a <sub>5</sub>
CO	300-1000	28.010	3.26E+00	1.51E-03	-3.88E-06	5.58E-09	-2.47E-12
	1000 - 5000	28.010	3.03E+00	1.44E-03	-5.63E-07	1.02E-10	-6.91E-15
CO <sub>2</sub>	300-1000	44.011	2.28E+00	9.92E-03	-1.04E-05	6.87E-09	-2.12E-12
	1000 - 5000	44.011	4.45E+00	3.14E-03	-1.28E-06	2.39E-10	-1.67E-14
O <sub>2</sub>	300-1000	31.999	3.21E+00	1.13E-03	-5.76E-07	1.31E-09	-8.77E-13
	1000 - 5000	31.999	3.70E+00	6.14E-04	-1.26E-07	1.78E-11	-1.14E-15
NO	300-1000	30.006	3.38E+00	1.25E-03	-3.30E-06	5.22E-09	-2.45E-12
	1000 - 5000	30.006	3.25E+00	1.27E-03	-5.02E-07	9.17E-11	-6.28E-15
N <sub>2</sub>	300-1000	28.013	3.30E+00	1.41E-03	-3.96E-06	5.64E-09	-2.44E-12
	1000 - 5000	28.013	2.93E+00	1.49E-03	-5.68E-07	1.01E-10	-6.75E-15

$$R_u = 8.315$$

$$\text{Residual MW} = 29.07$$

=

$$R(\text{Resid}) = 0.286$$

Residual masses

	CO	CO <sub>2</sub>	O <sub>2</sub>	NO	N <sub>2</sub>	Total
%	0.03	0.22	20.6	0.000495	79.85049	
					5	
mass	9.37E-07	6.87E-06	6.43E-04	1.55E-08	2.49E-03	3.12E-05

$$c_p(T) = 1.127 \times 10^{-17} T^4 - 5.62 \times 10^{-14} T^3 - 7.16 \times 10^{-11} T^2 + 8.12 \times 10^{-7} T + 0.0029$$

$$c_v(T) = 1.127 \times 10^{-17} T^4 - 5.62 \times 10^{-14} T^3 - 7.16 \times 10^{-11} T^2 + 8.12 \times 10^{-7} T + 0.0020$$

c<sub>p</sub> values

Temp	CO	CO <sub>2</sub>	O <sub>2</sub>	NO	N <sub>2</sub>	c <sub>p</sub> *MW
300	1.04E+00	8.47E-01	9.17E-01	9.91E-01	1.04E+00	3.19E-03
400	1.05E+00	9.38E-01	9.44E-01	1.00E+00	1.05E+00	3.23E-03
500	1.07E+00	1.01E+00	9.72E-01	1.02E+00	1.06E+00	3.27E-03
600	1.09E+00	1.08E+00	1.00E+00	1.04E+00	1.07E+00	3.33E-03
700	1.11E+00	1.13E+00	1.03E+00	1.06E+00	1.10E+00	3.40E-03
800	1.14E+00	1.17E+00	1.06E+00	1.09E+00	1.12E+00	3.48E-03
900	1.16E+00	1.21E+00	1.08E+00	1.12E+00	1.15E+00	3.56E-03
1000	1.19E+00	1.24E+00	1.09E+00	1.14E+00	1.17E+00	3.63E-03
1100	1.20E+00	1.26E+00	1.10E+00	1.15E+00	1.19E+00	3.68E-03
1200	1.22E+00	1.28E+00	1.11E+00	1.16E+00	1.20E+00	3.73E-03
1300	1.23E+00	1.29E+00	1.12E+00	1.17E+00	1.22E+00	3.77E-03
1400	1.25E+00	1.31E+00	1.13E+00	1.18E+00	1.23E+00	3.81E-03
1500	1.26E+00	1.32E+00	1.14E+00	1.19E+00	1.24E+00	3.84E-03
1600	1.27E+00	1.34E+00	1.15E+00	1.20E+00	1.25E+00	3.88E-03
1700	1.27E+00	1.35E+00	1.16E+00	1.21E+00	1.26E+00	3.90E-03
1800	1.28E+00	1.36E+00	1.17E+00	1.21E+00	1.27E+00	3.93E-03
1900	1.29E+00	1.37E+00	1.17E+00	1.22E+00	1.28E+00	3.95E-03
2000	1.30E+00	1.37E+00	1.18E+00	1.22E+00	1.28E+00	3.98E-03
2100	1.30E+00	1.38E+00	1.19E+00	1.23E+00	1.29E+00	3.99E-03
2200	1.31E+00	1.39E+00	1.20E+00	1.23E+00	1.30E+00	4.01E-03
2300	1.31E+00	1.39E+00	1.20E+00	1.23E+00	1.30E+00	4.03E-03
2400	1.31E+00	1.39E+00	1.21E+00	1.24E+00	1.30E+00	4.04E-03
2500	1.32E+00	1.40E+00	1.22E+00	1.24E+00	1.31E+00	4.06E-03
2600	1.32E+00	1.40E+00	1.22E+00	1.24E+00	1.31E+00	4.07E-03
2700	1.32E+00	1.41E+00	1.23E+00	1.24E+00	1.31E+00	4.08E-03
2800	1.32E+00	1.41E+00	1.23E+00	1.25E+00	1.32E+00	4.09E-03
2900	1.33E+00	1.41E+00	1.24E+00	1.25E+00	1.32E+00	4.10E-03
3000	1.33E+00	1.41E+00	1.25E+00	1.25E+00	1.32E+00	4.11E-03
3100	1.33E+00	1.42E+00	1.25E+00	1.25E+00	1.32E+00	4.12E-03
3200	1.33E+00	1.42E+00	1.26E+00	1.25E+00	1.33E+00	4.13E-03
3300	1.33E+00	1.42E+00	1.26E+00	1.25E+00	1.33E+00	4.14E-03
3400	1.34E+00	1.42E+00	1.27E+00	1.25E+00	1.33E+00	4.14E-03
3500	1.34E+00	1.43E+00	1.27E+00	1.26E+00	1.33E+00	4.15E-03

c<sub>v</sub> values

Temp	CO	CO <sub>2</sub>	O <sub>2</sub>	NO	N <sub>2</sub>	c <sub>v</sub> *MW
300	0.741356	0.65819	0.65684	0.713916	0.741169	2.28E-03
400	0.75403	0.748987	0.684313	0.726209	0.749881	2.32E-03
500	0.769172	0.823827	0.712568	0.741749	0.761175	2.36E-03
600	0.788791	0.886175	0.741192	0.76189	0.777263	2.42E-03
700	0.813131	0.938533	0.769227	0.786358	0.798611	2.49E-03
800	0.840672	0.982447	0.795167	0.813255	0.823946	2.57E-03
900	0.868132	1.018498	0.816958	0.839054	0.850253	2.65E-03
1000	0.890465	1.046311	0.832001	0.858602	0.872776	2.72E-03
1100	0.907246	1.068425	0.842464	0.872185	0.890498	2.77E-03
1200	0.922382	1.088235	0.852535	0.884413	0.906532	2.82E-03
1300	0.935996	1.105925	0.862232	0.895389	0.921002	2.86E-03
1400	0.94821	1.121672	0.871574	0.905215	0.934028	2.90E-03
1500	0.959137	1.135645	0.880581	0.913985	0.945725	2.93E-03
1600	0.968888	1.148007	0.889269	0.921793	0.956203	2.97E-03
1700	0.977568	1.158911	0.897654	0.928725	0.965567	2.99E-03
1800	0.985278	1.168503	0.905754	0.934866	0.973918	3.02E-03
1900	0.992112	1.176923	0.913582	0.940294	0.981351	3.04E-03
2000	0.99816	1.184302	0.921154	0.945086	0.987957	3.07E-03
2100	1.003509	1.190764	0.928484	0.949311	0.993822	3.09E-03
2200	1.008239	1.196424	0.935584	0.953038	0.999028	3.10E-03
2300	1.012425	1.201393	0.942468	0.956328	1.00365	3.12E-03
2400	1.016138	1.20577	0.949146	0.959241	1.007761	3.13E-03
2500	1.019443	1.209649	0.95563	0.96183	1.011426	3.15E-03
2600	1.022402	1.213117	0.961931	0.964146	1.014709	3.16E-03
2700	1.02507	1.216251	0.968057	0.966235	1.017666	3.17E-03
2800	1.027498	1.219123	0.974018	0.968139	1.020349	3.18E-03
2900	1.029733	1.221795	0.979822	0.969895	1.022806	3.19E-03
3000	1.031815	1.224324	0.985476	0.971537	1.02508	3.20E-03
3100	1.03378	1.226758	0.990988	0.973095	1.027208	3.21E-03
3200	1.03566	1.229136	0.996362	0.974592	1.029225	3.22E-03
3300	1.037481	1.231493	1.001605	0.976052	1.031157	3.23E-03
3400	1.039265	1.233853	1.006722	0.977489	1.033028	3.23E-03
3500	1.041028	1.236235	1.011715	0.978917	1.034858	3.24E-03

## APPENDIX C. FIGE VISUAL BASIC CODE

*“Public” and “Dim” statements are used to declare variables which will be used in the code.*

*An underscore character (\_) at the end of a line indicates the line is continued on the next line.*

```
Public CAInject, RPM As Integer
Public TsMax, TsMin As Double
Public Bore, Patm As Single
Public ClearArea, PistonHeadArea, ClearVol, TotalVol As Double
Public WorkingFluid As String
Public Resid_cp(1 To 5), Resid_cv(1 To 5), HeatCo(1 To 4) As Double
Public Ti, Vi, Pi As Double
Public Tf, T_end, m_Fuel As Double
```

*The next two lines declare object variables, used to improve the performance of the code.*

```
Dim FigeSheet, ConstSheet, DataSheet, ResidSheet, HeatSheet As Worksheet
Dim StartRange, Constants, DataPts, Residuals, Heat As Range
```

```
Dim Inject As String
Dim i, Index, ResIndex, HCIndex As Integer
Dim CA As Integer
Dim time1deg As Single
Dim Pf, P_Data As Double
Dim Vf, V_tot, V_liq, V_last As Double
Dim Tfs, T_new, delta_T As Double
Dim TsSlope, TsIntercept, Ts As Double
Dim mi, m_loss, initial_mass, delta_m_F As Double
Dim m_inj, m_last, m_air, m_liq, m_tot As Double
Dim initmass, m_Resid, CpTot As Double
Dim Gamma, rho_i, rr As Double
Dim Pressure(0 To 9), Volume(0 To 9) As Double
```

*The following sub-routine initializes all object variables.*

```
Sub InitObjVariables()
Set FigeSheet = Sheets("FIGE Calculation")
Set ConstSheet = Sheets("Engine Constants")
Set DataSheet = Sheets("Experimental Data")
Set ResidSheet = Sheets("Residuals")
Set HeatSheet = Sheets("HeatTransCoeff")
Set StartRange = FigeSheet.Range("B8")
Set Constants = ConstSheet.Range("B1")
Set DataPts = DataSheet.Range("A2")
Set Residuals = ResidSheet.Range("J4")
```

```
Set Heat = HeatSheet.Range("B39")
End Sub
```

*The following sub-routine retrieves constants that are contained in Excel spreadsheets and are based on the engine being modeled. These constants will be used later in the code.*

```
Sub GetConstantValues()
CAInject = Constants.Offset(1, 0) Crank angle at injection [deg]
TsMax = Constants.Offset(2, 0) max cylinder surface temp [K]
TsMin = Constants.Offset(3, 0) min cylinder surface temp [K]
RPM = Constants.Offset(4, 0) engine speed [rev/min]
Bore = Constants.Offset(5, 0) * 0.001 Engine bore [m]
ClearArea = Constants.Offset(6, 0) * 0.0001 Clearance area [m2]
PistonHeadArea = Constants.Offset(7, 0) * 0.0001 Piston head area [m2]
ClearVol = Constants.Offset(8, 0) * 0.000001 Clearance volume [m3]
TotalVol = Constants.Offset(9, 0) * 0.000001 Total Volume [m3]
Patm = Constants.Offset(10, 0) Atmospheric pressure [kPa]
WorkingFluid = Constants.Offset(11, 0) Vapor in the cylinder, air in this study
Ti = StartRange.Offset(0, 2) initial temp [K]
Vi = StartRange.Offset(0, 1) * 0.000001 initial volume [m3]
Pi = StartRange.Offset(0, 0) initial pressure [kPa]
For ResIndex = 1 To 5
The following are coefficients for specific heat calculations.
    Resid_cp(ResIndex) = Residuals.Offset(0, ResIndex)
    Resid_cv(ResIndex) = Residuals.Offset(3, ResIndex)
Next ResIndex
For HCIndex = 1 To 4
The following are coefficients for heat transfer coefficient calculations.
    HeatCo(HCIndex) = Heat.Offset(0, HCIndex - 1)
Next HCIndex
End Sub
```

*The following sub-routine is the main body of the FIGE code; it does the major calculations and calls the other subroutines.*

```
Sub FIGE()
InitObjVariables Calls the InitObjVariables subroutine
GetConstantValues Calls the GetConstantValues subroutine
```

*The following section sets up the spreadsheet for executing the FIGE process.*

```
FigSheet.Select
FigSheet.Range("D4:D5,B9:B5000,D9:E5000,G9:I5000").ClearContents
FigSheet.Range("C:C").Select
Index = WorksheetFunction.Count(Selection)
Range("A1").Select
```

*The following section is where the calculations are performed.*

$\text{time1deg} = 1 / (\text{RPM} * 6)$  Calculation for the time required for the piston to move through one crank angle degree.

The following two equations are used to calculate the cylinder surface temp.

$$\text{TsSlope} = (\text{TsMax} - \text{TsMin}) / (\text{ClearVol} - \text{TotalVol})$$

$$\text{TsIntercept} = \text{TsMax} - (\text{TsSlope} * \text{ClearVol})$$

The following six lines initialize variables to zero or the null character.

$\text{m\_loss} = 0$

$\text{m\_liq} = 0$

$\text{m\_Fuel} = 0$

$\text{m\_Resid} = 0$

$\text{P\_Data} = 0$

$\text{Inject} = ""$

$\text{initmass} = \text{Pi} * \text{Vi} / (\text{Rvalue}(\text{WorkingFluid}) * \text{Ti})$  Calculation of initial in-cylinder mass.

The next two lines calculate residuals left in the cylinder.

$\text{mi} = \text{initmass} * 0.9$

$\text{m\_Resid} = \text{initmass} * 0.1$

The "For Loop" is used to step through and perform calculations on each successive crank angle.

For  $i = 0$  To  $\text{Index} - 2$

The following 5 lines retrieve the initial values from the spreadsheet and converts them to the proper units.

$\text{Ti} = \text{StartRange.Offset}(i, 2)$  Initial temp [K]

$\text{Pi} = \text{StartRange.Offset}(i, 0)$  Initial pressure [kPa]

$\text{Vi} = \text{StartRange.Offset}(i, 1) * 0.000001$  Initial volume [ $\text{m}^3$ ]

$\text{Vf} = \text{StartRange.Offset}(i + 1, 1) * 0.000001$  Final volume [ $\text{m}^3$ ]

$\text{CA} = \text{StartRange.Offset}(i, -1)$  Crank angle

$\text{m\_tot} = \text{mi} + \text{m\_Fuel} + \text{m\_Resid}$  Calculation of total mass in the cylinder.

The following "If Statement" uses the "mass\_loss" function to calculate the mass loss due to leaks in the cylinder.

If  $\text{Pi} > \text{Patm}$  Then

$\text{m\_loss} = \text{mass\_loss}(\text{Pi})$

$\text{mi} = \text{mi} - (\text{m\_loss} * (\text{mi} / \text{m\_tot}))$

$\text{m\_Fuel} = \text{m\_Fuel} - (\text{m\_loss} * (\text{m\_Fuel} / \text{m\_tot}))$

$\text{m\_Resid} = \text{m\_Resid} - (\text{m\_loss} * (\text{m\_Resid} / \text{m\_tot}))$

$\text{m\_tot} = \text{mi} + \text{m\_Fuel} + \text{m\_Resid}$

End If

The following three calculations are heat transfer equations, which account for the difference in temperature between the mixture in the cylinder and the cylinder walls.

$\text{Ts} = ((\text{TsSlope} * \text{Vi} + \text{TsIntercept}) + \text{TsMax}) / 2$  Wall surface temp

$\text{CpTot} = (\text{CpMix}(\text{Ti}, \text{Ti}, \text{WorkingFluid}, \text{Inject}, \text{mi}, \text{m\_Fuel}) * (\text{mi} + \text{m\_Fuel}) + \text{m\_Resid} * \text{CpResid}(\text{Ti}, \text{Ti})) / \text{m\_tot}$  Specific heat of the mixture.

$\Delta T = ((\text{HeatTransCoeff}(\text{CA}) * \text{time1deg}) / (\text{m\_tot} * \text{CpTot})) * (((4 * (\text{Vi} - \text{ClearVol}) / \text{Bore}) * (\text{Ts} - \text{Ti})) + (\text{ClearArea} * (\text{TsMax} - \text{Ti})) + (\text{PistonHeadArea} * (\text{TsMin} - \text{Ti})))$  *Change in temp due to heat transfer.*  
 $\text{Ti} = \text{Ti} - \Delta T$  *Heat loss equation.*

*The following equation uses the “PressCalc” function to calculate the total pressure in the cylinder as a function of the partial pressures of the three substances.*

$\text{Pi} = \text{PressCalc}(\text{mi}, \text{WorkingFluid}, \text{Ti}, \text{Vi}) + \text{PressCalc}(\text{m\_Fuel}, \text{Inject}, \text{Ti}, \text{Vi}) + \text{PressCalc}(\text{m\_Resid}, \text{"Resid"}, \text{Ti}, \text{Vi})$   
 $\text{Tfs} = \text{Ti}$  *Assumed final temp.*

*The following “Do Loop” is the FIGE Process*

Do  
      $\text{Tf} = \text{Tfs}$   
      $\text{Gamma} = \text{GammaAveMix}(\text{Ti}, \text{Tf}, \text{WorkingFluid}, \text{Inject}, \text{mi}, \text{m\_Fuel}, \text{m\_Resid})$   
      $\text{Pf} = \text{Pi} * (\text{Vi} / \text{Vf}) ^ \text{Gamma}$   
      $\text{Tfs} = \text{Pf} * \text{Vf} * \text{Ti} / (\text{Pi} * \text{Vi})$   
 Loop While Abs( $\text{Tfs} - \text{Tf}$ ) > 0.000001

*The following “If Statement” calls the Injection sub-routine if injection has occurred or if there is liquid fuel in the cylinder.*

If  $\text{m\_liq} < 0$  Or  $\text{CA} + 1 = \text{CAInject}$  Then  
      $\text{P\_Data} = \text{DataPts.Offset}(i + 1, 1)$   
      $\text{T\_end} = 0$   
     Injection  
      $\text{m\_Fuel} = \text{m\_Fuel} + \Delta \text{m\_F}$   
      $\text{Tf} = \text{T\_end}$   
      $\text{Gamma} = \text{GammaAveMix}(\text{Ti}, \text{Tf}, \text{WorkingFluid}, \text{Inject}, \text{mi}, \text{m\_Fuel}, \text{m\_Resid})$   
      $\text{Pf} = \text{Pi} * (\text{Vi} / \text{Vf}) ^ \text{Gamma}$   
 End If

*The following lines of code output the calculated values to the spreadsheet.*

$\text{StartRange.Offset}(i + 1, 9) = \text{m\_Resid}$   
 $\text{StartRange.Offset}(i + 1, 7) = \text{m\_liq}$   
 $\text{StartRange.Offset}(i + 1, 6) = \text{mi}$   
 $\text{StartRange.Offset}(i + 1, 5) = \text{m\_Fuel}$   
 $\text{StartRange.Offset}(i + 1, 3) = \text{Gamma}$   
 $\text{StartRange.Offset}(i + 1, 2) = \text{Tf}$   
 $\text{StartRange.Offset}(i + 1, 0) = \text{Pf}$   
 Next i  
 End Sub

*The following sub-routine uses the Bisection method to calculate the mass of the evaporated fuel.*

Sub Injection()  
      $\text{Inject} = \text{Constants.Offset}(12, 0)$

```

m_inj = StartRange.Offset(i + 1, 4)
m_liq = m_inj + m_liq
m_min = 0.000000000001
m_max = m_liq

```

*The “Do Loop” is the Bisection method.*

```

Do
fa = massFunction(m_min)
m_mid = (m_min + m_max) / 2
f_mid = massFunction(m_mid)
If (fa * f_mid) > 0 Then
    m_min = m_mid
Else
    m_max = m_mid
End If
Loop Until (m_max - m_min) < 0.000000001
delta_m_F = m_mid
m_liq = m_liq - delta_m_F
If m_liq < 0.0000001 Then
    m_liq = 0
End If
End Sub

```

*The remainder of this appendix is a list of functions called by the sub-routines to perform repetitive calculations.*

*The “massFunction” function is used by the Bisection method to calculate the evaporated mass.*

```

Function massFunction(mass)
CpTot = (CpMix(Tf, Tf, WorkingFluid, Inject, mi, m_Fuel) * (mi + m_Fuel) _
    + m_Resid * CpResid(Tf, Tf)) / (m_Resid + mi + m_Fuel)
m_tot = mi + m_Resid + m_Fuel
T_end = Tf + ((HeatTransCoeff(CA) * time1deg * _
    (((4 * (Vi - ClearVol) / Bore) * (Tf - Ts)) + _
    (ClearArea * (Tf - TsMax)) + (PistonHeadArea * (Tf - TsMin)))) / _
    (m_tot * CpTot)) + ((mass * Lv(Inject)) / (m_tot * CpTot))
massFunction = ((mi * Rvalue(WorkingFluid) + _
    m_Resid * Rvalue(Resid) + mass * Rvalue(Inject)) * T_end / Vf) - _
    P_Data
End Function

```

*The “Rvalue” function returns a gas constant for a specific substance. Units kJ/kg-K.*

```

Function Rvalue(substance)
Select Case substance
Case "Air"
    Rvalue = 0.287

```



```

Case "Isooctane"
    Rvalue = 0.0728
Case "Resid"
    Rvalue = 0.286
End Select
End Function

```

*The "CpAve" function returns the average specific heat of a substance that has changed from state 1 to state 2. Units kJ/kg-K*

```

Function CpAve(T1, T2, substance)
Dim RangeB3 As Range
Set RangeB3 = Sheets("CurveFits").Range("B2")
Select Case substance
    Case "Air"
        a = RangeB3.Offset(0, 0)
        b = RangeB3.Offset(0, 1)
        c = RangeB3.Offset(0, 2)
        d = RangeB3.Offset(0, 3)
        e = RangeB3.Offset(0, 4)
        If T1 = T2 Then
CpAve = a + b * T1 + c * T1 ^ 2 + d * T1 ^ 3 + e * T1 ^ 4
        Else
CpAve = (a * (T2 - T1) + (b / 2) * (T2 ^ 2 - T1 ^ 2) + (c / 3) * (T2 ^ 3 - T1 ^ 3) + (d / 4) * (T2 ^ 4 - T1 ^ 4) + (e / 5) * (T2 ^ 5 - T1 ^ 5)) / (T2 - T1)
        End If
    Case "Isooctane"
        a = RangeB3.Offset(3, 0)
        b = RangeB3.Offset(3, 1)
        c = RangeB3.Offset(3, 2)
        d = RangeB3.Offset(3, 3)
        e = RangeB3.Offset(3, 4)
        If T1 = T2 Then
CpAve = a + b * T1 + c * T1 ^ 2 + d * T1 ^ 3 + e * T1 ^ -2
        Else
CpAve = (a * (T2 - T1) + (b / 2) * (T2 ^ 2 - T1 ^ 2) + (c / 3) * (T2 ^ 3 - T1 ^ 3) + (d / 4) * (T2 ^ 4 - T1 ^ 4) + (e * ((1 / T1) - (1 / T2)))) / (T2 - T1)
        End If
End Select
End Function

```

*The "GammaAveMix" function returns the average specific heat ratio of a mixture of substances, which have changed from state 1 to state 2.*

```

Function GammaAveMix(T1, T2, Sub1, Optional Sub2, Optional mass1, Optional mass2, Optional mass3)
mass3 is the mass of the residuals
If IsMissing(Sub2) Then
    CpM = CpAve(T1, T2, Sub1)

```

```

    CvM = CpM / Rvalue(Sub1)
Else
    Cp1 = CpAve(T1, T2, Sub1)
    Cp2 = CpAve(T1, T2, Sub2)
    Cv1 = Cp1 / Rvalue(Sub1)
    Cv2 = Cp2 / Rvalue(Sub2)
    If IsMissing(mass3) Then
        CpM = (mass1 * Cp1) + (mass2 * Cp2)
        CvM = (mass1 * Cv1) + (mass2 * Cv2)
    Else
        Cp3 = CpResid(T1, T2)
        Cv3 = CvResid(T1, T2)
        CpM = (mass1 * Cp1) + (mass2 * Cp2) + (mass3 * Cp3)
        CvM = (mass1 * Cv1) + (mass2 * Cv2) + (mass3 * Cv3)
    End If
End If
GammaAveMix = CpM / CvM
End Function

```

*The “Lv” function returns the latent heat of vaporization of a substance. Units kJ/kg.*

```

Function Lv(substance)
Select Case substance
    Case "Isooctane"
        Lv = 290
End Select
End Function

```

*The “CpMix” function returns the specific heat of a mixture, which has changed from state 1 to state 2. Units kJ/kg-K*

```

Function CpMix(T1, T2, Sub1, Sub2, mass1, mass2)
CpMix = (mass1 * CpAve(T1, T2, Sub1) + mass2 * CpAve(T1, T2, Sub2)) / _
    (mass1 + mass2)
End Function

```

*The “HeatTransCoeff” function returns the heat transfer coefficient for any given crank angle. Units mW/m<sup>2</sup>K.*

```

Function HeatTransCoeff(CrankAngle)
Select Case CrankAngle
    Case Is > 240
        HeatTransCoeff = (HeatCo(1) * CrankAngle ^ 3 + HeatCo(2) * CrankAngle ^ 2 + _
HeatCo(3) * CrankAngle + HeatCo(4))
    Case Is <= 240
        HeatTransCoeff = 90 * 0.001
End Select
End Function

```

*The “mass\_loss” function returns the mass loss due to leaks in the piston-cylinder assembly. Units kg.*

Function mass\_loss(Press)

Select Case Press

Case Is <= 1260

mass\_loss = -1.27268E-12 \* Press ^ 2 + 1.1340981E-09 \* Press + 0.0000005939022

Case Is > 1260

mass\_loss = 0

End Select

End Function

*The “PressCalc” function returns the pressure of a gaseous substance at a specific state. Units kPa.*

Function PressCalc(mass, subs, Temp, Vol)

PressCalc = mass \* Rvalue(subs) \* Temp / Vol

End Function

*The “CpResid” function returns an average specific heat at constant pressure for the residuals in the cylinder. Units kJ/kg-K.*

Function CpResid(temp1, temp2)

If temp1 = temp2 Then

CpResid = Resid\_cp(5) + Resid\_cp(4) \* temp1 + Resid\_cp(3) \* temp1 ^ 2 + \_

Resid\_cp(2) \* temp1 ^ 3 + Resid\_cp(1) \* temp1 ^ 4

Else

CpResid = (Resid\_cp(5) \* (temp2 - temp1) + (Resid\_cp(4) / 2) \* (temp2 ^ 2 - temp1 ^ 2) \_  
+ (Resid\_cp(3) / 3) \* (temp2 ^ 3 - temp1 ^ 3) + (Resid\_cp(2) / 4) \* (temp2 ^ 4 - \_ temp1 ^ 4)  
+ (Resid\_cp(1) / 5) \* (temp2 ^ 5 - temp1 ^ 5)) / (temp2 - temp1)

End If

End Function

*The “CvResid” function returns an average specific heat at constant volume for the residuals in the cylinder. Units kJ/kg-K.*

Function CvResid(temp1, temp2)

If temp1 = temp2 Then

CvResid = Resid\_cv(5) + Resid\_cv(4) \* temp1 + Resid\_cv(3) \* temp1 ^ 2 + Resid\_cv(2) \_  
\* temp1 ^ 3 + Resid\_cv(1) \* temp1 ^ 4

Else

CvResid = (Resid\_cv(5) \* (temp2 - temp1) + (Resid\_cv(4) / 2) \* (temp2 ^ 2 - temp1 ^ 2) \_  
+ (Resid\_cv(3) / 3) \* (temp2 ^ 3 - temp1 ^ 3) + (Resid\_cv(2) / 4) \* (temp2 ^ 4 - \_ temp1  
^ 4) + (Resid\_cv(1) / 5) \* (temp2 ^ 5 - temp1 ^ 5)) / (temp2 - temp1)

End If

End Function